

Document downloaded from:

<http://hdl.handle.net/10251/200800>

This paper must be cited as:

Silva-Gaspar, B.; Martínez-Franco, R.; Pirngruber, G.; Fécant, A.; Díaz Morales, UM.; Corma Canós, A. (2022). Open-Framework Chalcogenide Materials - from isolated clusters to highly ordered structures - and their photocatalytic applications. *Coordination Chemistry Reviews*. 453:1-54. <https://doi.org/10.1016/j.ccr.2021.214243>



The final publication is available at

<https://doi.org/10.1016/j.ccr.2021.214243>

Copyright Elsevier

Additional Information

Cluster-based Chalcogenide Materials for Photocatalysis
Applications
Draft

Beatriz Silva Gaspar

April 10, 2020

Contents

1	Introduction	2
2	Microporous Oxides vs. Microporous Chalcogenides	3
3	Tetrahedral Clusters	3
3.1	Supertetrahedral Clusters T_n	3
3.1.1	T2 and T3 based chalcogenide materials.....	5
3.1.2	Supertetrahedral clusters with $n > 3$	8
3.2	Super-supertetrahedral Clusters $T_{p,q}$	12
3.3	Pentasupertetrahedral Clusters P_n	13
3.4	Capped Supertetrahedral Clusters C_n	14
3.5	Oxyclusters	15
3.6	TON series	16
3.7	Structures with different series and types of clusters	17
4	Non Tetrahedral Clusters	18
4.1	Semi-cube Clusters	18
4.2	Icosahedral Clusters	19
5	Zeolite Analogue Structures	21
6	Hydrated Open Framework Chalcogenides	27
7	Hybrid Materials	30
8	Alternative Methods of Synthesis	33
8.1	Ionothermal Syntheses.....	33
8.2	Surfactant-thermal Method.....	37

1 Introduction

In recent years intensive research has been carried out in the area of photocatalysis as a form of degradation of polluting compounds, but also as an alternative to the production of fuels. The first compound found to show photocatalytic activity was TiO_2 in 1972 [1], and since then, different ways to increase photocatalytic performance have been investigated. Different materials, such as metal oxides, metal and oxy-nitrides, metal chalcogenides, alkali metal base, Z-scheme systems and organic materials, are being investigated for use as photocatalysts. Of the materials presented, the metal oxides, metal chalcogenides and their composites stand out [2].

The vast majority of oxides show high values for the optical band gap and can only absorb radiation in the UV region. Bearing in mind that only 5% of the solar spectrum is made up of UV radiation and about 43% of the visible radiation, the synthesis of materials with band gaps more adapted to solar radiation becomes essential [3]. Metal chalcogenides comprise a viable alternative to metal oxides, as they have a band gap more suitable for solar radiation [4]. It is already possible to find in the literature reference to the use of metal chalcogenides as photocatalysts in processes of pollutants degradation but also for the production of fuels [5] [6] [7] [8] [9] [10] [11] [12] [13].

Microporous materials have, over time, attracted an enormous interest in both scientific and technological fields. Since they allow the interaction with atoms, molecules and ions at the surface but also at the bulk, these materials have innumerable applications, namely in gas separation, ionic exchange and petrochemical industries [14]. Since the applications of these materials are closely related to their chemical composition and topology, intense research has been carried out on the synthesis of new materials. According to Zheng et al. [15] there are several advantages in using crystalline microporous materials as active photocatalysts. The open framework architecture helps increase the number of active sites due to the high surface area, but also it is likely to reduce the electron-hole recombination rate since it reduces the average carrier path to reach the surface of the catalysts particle where the reaction occurs. However, oxide based porous materials are insulators, presenting limitations in their applications. Thus, in order to expand such applications, the synthesis of porous materials with properties of a semiconductor became desirable [16].

Recently, porous chalcogenides materials have received special attention, as they combine the presence of an open framework with semiconductivity, thus making it possible to use such materials in optoelectronic devices, photocatalysis and fast ionic conduction materials [17].

Although it is possible to find in the literature numerous reviews about metal chalcogenide materials, notably on metal sulfide nanostructures [18] [19], hollow nanostructures [20], nanocrystals [21], composites with graphene [22] and more recently on the application of metal sulfides on water splitting for H_2 production [2], this review will focus on porous chalcogenides materials that have clusters as building blocks, because the most recent review on this subject

is from 2005 and major developments have happened since then [23].

This review is divided into two parts. The first part will focus on materials science, more specifically on presenting the differences between microporous oxides and microporous chalcogenides, followed by the presentation of the main clusters that constitute these materials. After it, there is a reference to the materials that are made up by such clusters: structures analogous to zeolites, hydrated structures and ultimately hybrid materials. To finish the section on materials science, two alternatives of synthesis that have been investigated recently are presented. The second part will focus on photocatalysis, in particular the application of these materials to the degradation of pollutants or the production of hydrogen or value added chemical compounds.

2 Microporous Oxides vs. Microporous Chalcogenides

A great and obvious distinction between both materials is the replacement of Oxygen by another chalcogen, such Sulphur, Selenium or Tellurium. Unlike Oxygen, it is possible for the others chalcogens to present a coordination 4. Thus, the microporous chalcogenides can present cations and anions with tetrahedral coordination [23].

When the TO_4 tetrahedra of the framework of an oxide is replaced by the TX_4 ($X = S, Se$ or Te) tetrahedra, the framework tends to increase its density, since the T-X-T angle is lower than the T-O-T angle. In order to avoid such compaction, the tetrahedra TX_4 is replaced by a M_nS_n cluster, where M is a metal cation, generally from Groups 12-14 (such as Zn, Cd, Ga, In, Ge and Sn) [24]. Chalcogenide materials are therefore described as a network of clusters, presenting an extra structural level associated with each cluster. Of the many known clusters [25], the tetrahedrally shaped clusters that are able to form links through their vertices stand out.

Since the discovery in 1989 by Bedard et al. [26] [27] of microporous sulfides through hydro(solvo)thermal methods, intensive research has been carried out in order to obtain new materials with controlled chemical compositions and architectures, so that their physical and chemical properties are better adapted to a specific application [28].

3 Tetrahedral Clusters

3.1 Supertetrahedral Clusters T_n

The simplest and most common series of tetrahedral clusters are called supertetrahedral clusters. These clusters are fragments of the cubic ZnS-type lattice and denoted as T_n by Li et al. [29], where n represents the number of metal layers. The figure 1 shows the diagrams of different T_n clusters for $n=2, 3, 4, 5$.

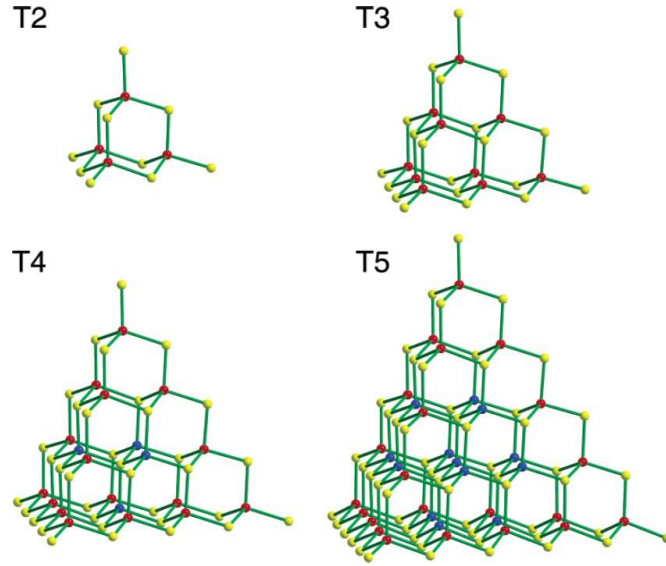


Figure 1: Diagrams for different T_n clusters ($n = 2, 3, 4$ and 5) where the red balls represent the cations and the yellow balls the anions. In clusters where two types of cations coexist, the blue balls represent the divalent cations [23]

The number of cations in a T_n cluster is given by $t_n = n(n+1)(n+2)/6$. The number of anions per cluster is given by $t_{n+1} = (n+1)(n+2)(n+3)/6$. The formulas for discrete T_n ($n = 2-6$) clusters are M_4X_{10} , $M_{10}X_{20}$, $M_{20}X_{35}$, $M_{35}X_{56}$ and $M_{56}X_{82}$, respectively. Taking into account that in a continuous network of clusters the four vertices of the supertetrahedron are shared with another supertetrahedron, the final composition of the structure is M_xX_y , where $x = t_n$ and $y = t_{n+1} - 2$. Regarding coordination, all cations have a coordination equal to 4. The same is no longer true for anions. They may have a coordination of 2 if they are at the vertices of the cluster, coordination of 3 if they are on the face of the cluster, or coordination of 4 if they are within the cluster. The number of anions with 2-coordination is given by $6n - 4$, with 3-coordination given by $2(n-1)(n-2)$ and with 4-coordination is given by $(n-3)(n-2)(n-1)/6$. The table 1 shows the number of cations and anions present in an isolated T_n cluster or when it participates in a network, as well as the number of anions with coordination 2, 3 and 4. It is observed that anions with 4-coordination only exist for n greater or equal to 4. In order to ensure the compliance with Brown's equal valence rule, the 4-coordinated chalcogen atoms are only bonded to divalent cations in order to ensure that the four bonds have a bond valence of $1/2$, thus explaining the need to use divalent cations to obtain clusters with n greater or equal to 4. The number of divalent cations in the cluster as a function of n is given by $t_n - 6n + 8$ [30] [31].

Table 1: Composition of T_n clusters

Cluster T_n	t_n	t_{n+1}	Number of Cations x	Number of Anions y	nation		
					2	3	4
1	1	4	1	2	2	0	0
2	4	10	4	8	8	0	0
3	10	20	10	18	14	4	0
4	20	35	20	33	20	12	1
5	35	56	35	54	26	24	4
6	56	84	56	82	32	40	10

3.1.1 T2 and T3 based chalcogenide materials

In 1994 Yaghi et al. [32] presented the first synthesis of an open framework microporous sulfide based on Ge containing the T2 Ge_4S_{10} cluster as building unit. In order to achieve the 3-dimensional structure it was necessary to add mono or divalent cations, such as Mn, Cu [33] [34] or Ag [35], which will be responsible for connecting the different building unit, hence avoiding the formation of a layered material. Therefore, the crystalline structure is based on the presence of Ge_4S_{10} clusters which are connected by MnS_4 tetrahedra. Also based on the T2 Ge_4S_{10} cluster, Cahill et. al [36] obtained a material entitled QUI-MnGS-1 with a diamond lattice. Although QUI-MnGS-1 is also based on Ge_4S_{10} cluster, the presence of MnS_4 tetrahedra is not observed. The connection between the Ge_4S_{10} clusters is made by means of sulphur bridges. It was observed that it is possible to eliminate part of the template through calcination at a temperature between 240°C and 360°C without destroying the framework. Another interesting structure was synthesised by Zheng et al. [37]. A laminar material was obtained, titled UCR-28, constituted by alternating T2 $Ge_3S_9Zn(H_2O)$ clusters and simple $ZnS_3(H_2O)$ tetrahedrons. In UCR-28 the $Zn(C_6N_4H_{18})(H_2O)$ complex ion is used as structuring directing agent instead of an organic amine or a pure organic cations.

In the Ge-S system the largest synthesised cluster was type T2. This is justified by the fact that the cations charge is too high to satisfy the anion coordination environment [38]. The number of known 3D frameworks is low, since an M^{4+} -S network would be neutral, not allowing the electrostatic interaction with a structuring agent [23].

The chemical system In-S have been extensively studied by Cahill et al. [24] [39]. Several materials with different dimensions, from OD to 3D, based on the T2 In_4S_{10} and T3 $In_{10}S_{20}$ clusters were obtained. As for the materials based on the T3 clusters, it was concluded that such cluster could be obtained over a range of templates, and the presence of water played an important role in defining the final topology of the material, but not on the type of cluster formed (see table 2). Therefore, it can be said that the template is not the only one responsible for the final topology of the material.

Li et al. [29] [40] also synthesised 3D microporous solids based on In. The synthesised structure presents the T3 clusters as building units. Three crystalline structures, ASU-31,

ASU-32 and ASU-34, were obtained, because different types of structuring agents were used. Comparing the structures obtained by Cahill [24] [39] and Li [29] [40] (see table 2), the structures synthesised by the first present an interpenetrated framework. This type of framework occurs when the pore size is too large to support the framework. This is not the case with the structures obtained by Li, since the templates used allowed to obtain the giant cavities.

Table 2: Different materials based on T3 $\text{In}_{10}\text{S}_{20}$ cluster and their gels compositions and final topology (adapted from [24])

Material	Template	Gel composition				Cluster	Structure	Interpenetration	Ref.
		In	S	Organic	H ₂ O				
DMA-InS-SB1	DMA ¹	1	2,3	4,4	16,6	T3	3D - DD ²	Yes	[39]
DEA-InS-SB1	DEA ³	1	2,3	6,8	trace	T3	3D - DD ²	Yes	[24]
DEA-InS-SB2	DEA ³	1	2,3	3,4	14,0	T3	2D	-	[24]
ASU-31	HPP ⁴	1	2,5	n/a	n/a	T3	3D - SOD ⁵	No	[29]
ASU-32	DPM ⁶	1	2,5	n/a	n/a	T3	3D - CrB ₄ ⁷	No	[29]
ASU-34	HMA ⁸	1	2,5	n/a	n/a	T3	3D - CrB ₄ ⁷	No	[40]

¹ Dimethylamine. ² Double Diamond (see figure 2a). ³ Diethylamine. ⁴ 1,3,4,6,7,8-hexahydro-2H-pyrimido[1,2-a]pyrimidine.

⁵ Sodalite (see figure 2b). ⁶ Dipiperidinomethane. ⁷ Cristobalite (see figure 2c). ⁸ Hexamethyleimine.

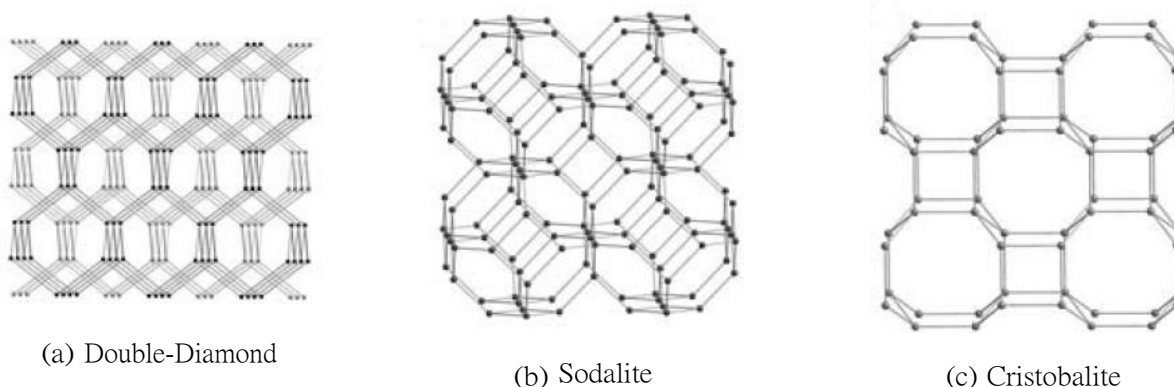


Figure 2: Representation of double-diamond (DD), sodalite (SOD) and cristobalite (CrB₄) topologies [38]

The Ga-S system was also studied. Zheng et al. [41] obtained for the first time a structure based on the T3 $\text{Ga}_{10}\text{S}_{18}$ cluster, titled UCR-7. Depending on the structuring agent used, they were able to obtain a structure based on cluster T3 $\text{Ga}_{10}\text{S}_{17,5}(\text{S}_3)_{0,5}$, entitled UCR-18, that presented for the first time a polysulfide linkage between the clusters.

More recently, a 3D structure based on the combination of Sn, In and S has been synthesised [42]. The synthesised material, entitled SCU-36, has as framework based on 3-connected T2 clusters and has a etc topology. Other interesting features about SCU-36 is the presence of extra large channels, consisting of 36-MR, and a very low framework density. As for the exchange properties of the material, after 12 hours of exchange with CsCl the N_2 absorption is negligible. When the time of exchange or the CsCl concentration were increased, the structure collapsed.

Based on the same chemical system, 2D structures were later obtained [43]. Such materials, entitled SOF-23 and SOF-24, are based on the presence of interrupted T3-InSnS clusters but present different connection modes between the different clusters. Although SOF-21 and SOF-22 have different topologies, both materials have the same bandgap value. Continuing the research to obtain more complex structures, Wang et al. [44] synthesised for the first time a structure based on the extended spiro-5 unit. The presence of the extended spiro-5 unit occurs through the fusion of 5 T3-InSnS clusters. The obtained compound, entitled SOF-27, presents for the first time a NAB topology. Comparing the structure obtained with nabasetie, the only known zeolite with the NAB structure, the ring size is increased 3 times due to the use of T3 clusters at the expense of TO₄, thus showing the consequences of using T_n clusters as building units in the pore size.

Turning to selenium-based materials, there is a reduced number of crystalline 3D selenium-based frameworks. The first known structure is based on the T2 cluster Ge₄Se₁₀ where the addition of divalent metal cations is required to connect the different clusters in order to achieve a 3D framework [45].

Continuing the search for larger clusters, the first T3 cluster based on the In-Se system was obtained by Wang et al. [46]. Later, Xue et al. [47] were able to obtain a family of compounds also based on the In-Se which presented polyselenides linkers as a way to connect the different clusters.

As for the Ga-Se chemical system, the first 3D open frameworks based on T3 clusters as building units were first obtained by Bu et al. [48]. Two different materials were obtained: OCF-6 and OCF-13. The first one presents a diamond topology and a ring size of 18 while the second one presents a cristobalite topology and a ring size of 24. The synthesised structures present noninterpenetrating frameworks while the ones obtained for the Ga-S system are all interpenetrating nets. As for the synthesis conditions, the presence of water promotes the crystal growth while in the Ga-S system the synthesis must be held in a nonaqueous medium. Regarding the band gap value, the Ga-Se structures have a band gap below 2eV, something that is not observed in the Ga-S structures (see table 3). The analysis of the table 3 also shows that two structures composed by the same type of clusters but with different topologies have different bandgap. Therefore, in the Ga-X system (X = S, Se) the anion and topology influence the bandgap value.

Table 3: Different materials based on T3 Ga₁₀X₂₀ (X = S, Se) cluster and their gels compositions, final topology and band gap

Material	Template	Gel composition (mol)					Cluster	Structure	Interpenetration	Band gap (eV)	Ref.
		Ga	S	Se	Organic	H ₂ O					
UCR-7-GaS-TETA	TETA ¹	n/a	n/a	-	n/a	-	T3	3D	Yes	n/a	[41]
UCR-7-GaS-TAE	TAE ²	n/a	n/a	-	n/a	-	T3	3D	Yes	n/a	[41]
UCR-7-GaS-DBA	DBA ³	n/a	n/a	-	n/a	-	T3	3D	Yes	2,84	[41]
UCR-18-GaS-AEP	AEP ⁴	1	3,3	-	8,6	-	T3	3D	Yes	n/a	[41]
-	DEA ⁵	1	2,1	-	33,0	-	T3	3D - DD ⁶	Yes	4	[49]
OCF-6-GaSe-TMDP	TMDP ⁷	1	-	2,5	4,9	152,9	T3	3D - D ⁸	No	1,43	[48]
OCF-13-GaSe-DPM	DPM ⁹	1	-	2,5	5,2	207,5	T3	3D - CrB ₄ ¹⁰	No	1,76	[48]

¹ Triethylenetetramine. ² Tris(2-aminoethyl)amine. ³ Di-n-butylamine. ⁴ 1-(2-aminoethyl)piperazine. ⁵ Diethylamine. ⁶ Double Diamond (see figure 2a).

⁷ 4,4'-trimethylenedipiperidine. ⁸ Diamond (see figure 3). ⁹ Dipiperidinomethane. ¹⁰ Cristobalite (see figure 2c).

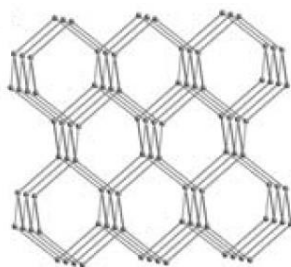


Figure 3: Representation of diamond (D) topology [38]

Regarding Tellurium, obtaining structures with this element is the most challenging, since Tellurium presents low reactivity and tellurides are environmentally unstable. Although examples of structures with Te are found in the literature, the majority do not present clusters as building units [50]. The first material based on T2 Ge/Sn-Te clusters was obtained by Tsamourtzzi et al. [51]. Following these works, Zhang et al [52] obtained the first material based on T2 In-Te clusters. The material obtained has a 2D chiral structure and the T2 clusters that compose it have a different composition than usual. One of the Te of the cluster was substituted by ethylenediamine. This organic component has a terminal position, not making any connection with other clusters.

3.1.2 Supertetrahedral clusters with $n > 3$

The need to obtain structures with large pores has led to the development of materials consisting of T n clusters with n greater than 3, since the size of the ring is increased n times, thus leading to structures with a highly open framework [48]. Although T n are the most commonly used type of clusters, there are some limitations in their use. The first is the way to connect the different clusters. Generally, the connection between two clusters is made through bi-coordinated chalcogen bridge. When using this type of clusters the formed structures tend to be interpenetrated, in order to reduce the potential energy and stabilise the structure, leading to a reduction in pore size and pore volume [53] [54]. Another difficulty that arises is the drastically increase of negative charges with increasing n , making it difficult to synthesise clusters with large

dimensions. As the cluster size increases, so does the surface area, leading to an increase in the number of unconnected S^{2-} atoms [55].

The first material based on a T4 cluster was synthesised in 2001 by Li et al. [30]. This interpenetrating structure is formed by clusters of the type $Cd_4In_{16}S_{33}$, where Cd^{2+} presents a fundamental role in obtaining such structure. It is due to the addition of the divalent cation that the local charge balance at the core tetrahedral anion is achieved. Continuing the research on the synthesis of structures based on T4 clusters, Bu et al. [53] managed to synthesise a structure where a sulphur atom was connecting three T4 clusters. Wang et al. [56] [57] was able to synthesise a family of T4-based noncentrosymmetric three-dimensional sulphides as well as using transition metals, such as Fe and Co, to join the different T4 clusters into a 2D-framework. Taking into account the mentioned materials (see table 4), it is possible to obtain the structure of cristobalite from a diverse range of templates, provided it contain a piperazine ring. However, the cubic carbon nitride and UCR-1 topologies are more rigid, since they can only be obtained from di-n-butylamine and 4,4'-trimethylenedipiperidine, respectively, as a template. It is also interesting to note that when using 1,2-diaminocyclohexane as a template in the chemical systems In-Fe-S or In-Co-S the final material presents a 2D structure instead of a 3D structure.

Table 4: Different materials based on T4 $In_{16}X_4S_{35}$ ($X = Zn, Cd, Fe, Co, Mn$) cluster and their gels compositions and final topology

Material	Template	Gel composition (mol)				Cluster	Structure	Interpenetration	Ref.
		In	S	X	Organic				
CdInS-44	BAPP ¹	1	2,5	0,3	4,3	$In_{16}Cd_4S_{35}$	3D - CrB_4^2	Yes	[30]
UCR-8FeInS-DBA	DBA ³	n/a	n/a	n/a	n/a	$In_{16}Fe_4S_{35}$	3D - $C_3N_4^4$	No	[53]
UCR-8CoInS-DBA	DBA ³	n/a	n/a	n/a	n/a	$In_{16}Co_4S_{35}$	3D - $C_3N_4^4$	No	[53]
UCR-8ZnInS-DBA	DBA ³	1	3,5	0,4	15,1	$In_{16}Zn_4S_{35}$	3D - $C_3N_4^4$	No	[53]
UCR-8CdInS-DBA	DBA ³	n/a	n/a	n/a	n/a	$In_{16}Cd_4S_{35}$	3D - $C_3N_4^4$	No	[53]
UCR-1CdInS	TMDP ⁵	1	2,9	0,3	3,9	$In_{16}Cd_4S_{35}$	3D - UCR-1 ⁶	No	[56]
UCR-1ZnInS	TMDP ⁵	n/a	n/a	n/a	n/a	$In_{16}Zn_4S_{35}$	3D - UCR-1 ⁶	No	[56]
UCR-1MnInS	TMDP ⁵	n/a	n/a	n/a	n/a	$In_{16}Mn_4S_{35}$	3D - UCR-1 ⁶	No	[56]
UCR-1CoInS	TMDP ⁵	n/a	n/a	n/a	n/a	$In_{16}Co_4S_{35}$	3D - UCR-1 ⁶	No	[56]
UCR-5ZnInS-1	BAPP ¹	n/a	n/a	n/a	n/a	$In_{16}Zn_4S_{35}$	3D - CrB_4^2	No	[56]
UCR-5ZnInS-2	AEPP ⁷	n/a	n/a	n/a	n/a	$In_{16}Zn_4S_{35}$	3D - CrB_4^2	No	[56]
UCR-5ZnInS-3	ATMP ⁸	n/a	n/a	n/a	n/a	$In_{16}Zn_4S_{35}$	3D - CrB_4^2	No	[56]
UCR-5MnInS	BAPP ¹	n/a	n/a	n/a	n/a	$In_{16}Mn_4S_{35}$	3D - CrB_4^2	No	[56]
UCR-5CoInS	BAPP ¹	n/a	n/a	n/a	n/a	$In_{16}Co_4S_{35}$	3D - CrB_4^2	No	[56]
-	DACH ⁹	1	2,0	0,5	132,9	$In_{16}Fe_4S_{35}$	2D	-	[57]
-	DACH ⁹	1	4,0	0,5	149,5	$In_{16}Co_4S_{35}$	2D	-	[57]

¹1,4-bis(3-aminopropyl)piperazine. ²Cristobalite (see figure 2c). ³Di-n-butylamine. ⁴Cubic carbon nitride (see figure 4a). ⁵4,4'-trimethylenedipiperidine.

⁶UCR-1 topology (see figure 4b). ⁷1-(2-aminoethyl)piperazine. ⁸4-amino-2,2,6,6-tetramethylpiperidine. ⁹1,2-diaminocyclohexane.

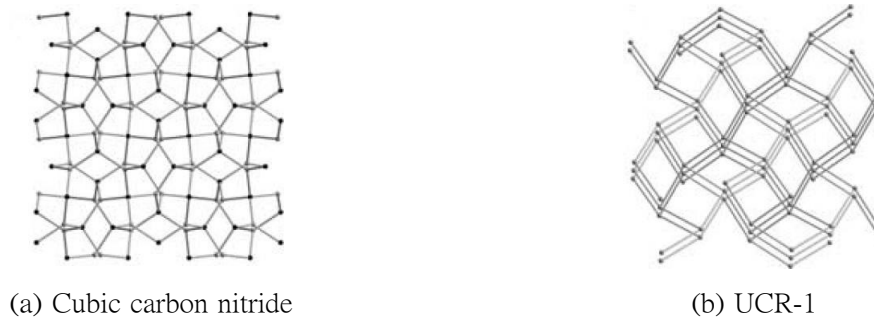


Figure 4: Representation of Cubic carbon nitride (C_3N_4) and UCR-1 topologies [38]

Now replacing In with Ga, Zheng et al. [41] were able to synthesise a structure based on the T4 $Zn_4Ga_{16}S_{33}$ clusters with the same structure, UCR-5, as the materials previously obtained by Wang et al. [56]. Continuing the study of materials containing Ga, Bu et al. [48] obtained a material based on the Ga-Zn-Se system that does not present a interpenetrating framework.

Wu et al. [55] managed to synthesise a family of materials based on the complex Sn-Ga-M-X ($M = Mn, Cu, Zn; W = S, Se$) chemical system. It was found that in the systems under study there was a phase transformation from a 3D interpenetrated diamond framework composed of T4 clusters, OCF-5, to isolated and highly stable T4 clusters, OCF-40.

It is well known that the doping of a material is used to tune its electronic properties. Wu et al. [58] evaluate how the doping of the chemical system Ga-Zn-Se by Sn or S or changing the amine type can influence the electronic properties of such T4 cluster based materials. The starting gel consisted of $Ga(NO_3)_3$, $Zn(NO_3)_2$, Se and H_2O . Four different templates, 1,5-diamino-2-methylpentane (DAMP), 4, 40-trimethylenedipiperdine (TMDP), piperidine (PR) or N-ethylcyclohexanamine (ECHA), were evaluated and for each template doping with Sn (by adding $SnCl_2$), S (by adding dimethylsulfoxide - DMSO) and dual doping with Sn and S was also evaluated. The experimental results of the different forms of doping are represented schematically in the figure 5.

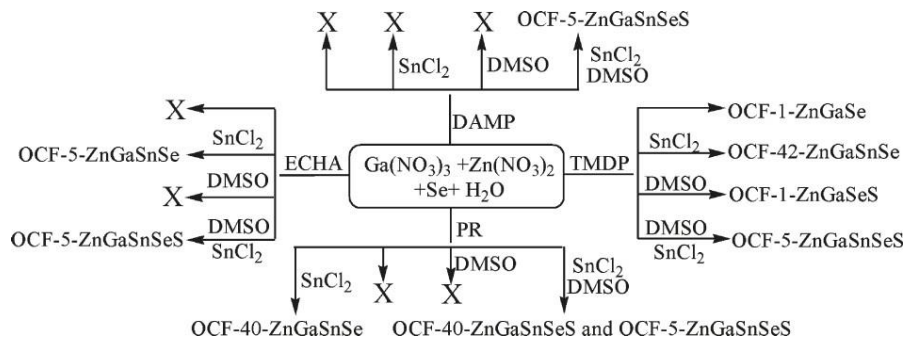


Figure 5: Schematic of the different forms of doping as well as the experimental results obtained (X means no crystalline product is obtained) [58]

Taking into account Pauling's valence rule and Pearson's hard and soft acid base theory, the core anion should be surrounded by Zn^{2+} and the corner sites should be occupied by high

valence cations. Such rules dictate the distribution of the different ions on the cluster. It was observed that the core Se^{2-} is easily replaced by S^{2-} and partial replacement of the Se^{2-} at the face sites by S^{2-} is observed. The doping with Sn^{4+} , which will substitute the Ga^{3+} at the corner sites, suppresses the doping by S^{2-} because it has a bigger affinity for Se^{2-} . Comparing the consequences of the doping on the charge of the cluster, doping with S^{2-} does not affect it while doping with Sn^{4+} reduces the global charge of the cluster. Therefore, organic amines with lower charge density induce more Sn^{4+} doping on the corner sites of the cluster. The doping also affects the cluster size. Taking into account ionic radii and bond distances, doping with Sn increases the size of the cluster and doping with S decreases it. No doping or only doping with S while using TMDP leads to OCF-1 (material previously studied by Bu et al. [48]). For all used amines OCF-5 (see [55] for more information regarding the topology) is obtained when both Sn and S doping is used. When only Sn doping is used OCF-5, OCF-40 or OCF-42 (OCF-42 is 3D structure composed by the combination of T2 and T4 clusters [59]) can be obtained, depending on the organic amine used. Regarding the optical properties of the obtained materials, it is observed that doping with Sn causes a red shift and doping with S leads to a blue shift. As for dual doped samples, the direction of the shift is related to which doping agent is dominant.

All 3D structures based on T4 clusters composed by three different metals have diamond as topology, regardless of the template used. It is also noted that the material with the lowest bandgap, 1.5 eV, is the OCF-5 structure composed by the combination Sn-Ga-Cu-Se.

Using the T4 isolated clusters formerly obtained by Wu et al. [55], Liu et al. [60] doped OCF-40 with Mn, Co or Zn in order to produce a photocatalyst for the electrochemical water splitting process.

The first synthesised T5 cluster had a missing core atom [61]. As there is no core atom, there are no sulphur atoms with 4-coordination, so the existence of divalent cations is not necessary. Thus, it is possible to achieve large-sized clusters without the need to incorporate divalent cations in the structure, provided that the clusters have at least one missing core atom. Other structures based on pseudo T5 clusters were synthesised. Su et al. [62] managed to obtain a layered structure based on pseudo T5 cluster $\text{In}_{28}\text{Cd}_6\text{S}_{56}$. The synthesised structure has a lower Cd content than the expected for a theoretical T5 cluster, as the theoretical $\text{In}_{22}\text{Cd}_{13}\text{S}_{54}$ cluster is unstable due to the high negative charges.

To synthesise a true T5 cluster it was necessary to add Cu to the In-S system, obtaining a cluster with the formula $\text{Cu}_5\text{In}_{30}\text{S}_{54}$ [63]. With this type of clusters it was possible to synthesise two distinct structures, one with a 2D framework, entitled UCR-16, and another with a 3D framework, the UCR-17.

Wu et al. [64], in order to study the insertion of dopants in specific places at atomic scale, obtained for the first time isolated T5 clusters. For that, a pseudo T5 cluster was first synthesised, entitled ISC-10, based on Cd-In-S system. It was also observed that, when the amount of Cd in the precursor gel increases, a 2D framework is obtained, entitled OCF-43, composed by the same clusters as in ISC-10. After obtaining the ISC-10, diffusion of Cu to the void of the cluster is performed, obtaining at the end a T5 cluster composed by Cu-Cd-In-S. The presence of the Cu at the void changes dramatically the electronic properties of the structure.

There is a red shift on the band gap due to the Cu. As for the generation and separation of photoinduced electron-hole pair, the sample doped with Cu presents a higher photocurrent density. Therefore, even a small amount of Cu is enough to cause big differences on the photoelectric properties of the materials. The doping of ISC-10 by Mn^{2+} was also evaluated [65]. Comparing both dopings, Mn^{2+} has a minor impact on the band gap of the material. However, after the doping with Mn^{2+} there is a strong red emission that is not observed in the typical semiconductor materials doped with Mn^{2+} .

Of the T5 clusters obtained so far only the combination $\text{M}^{3+}/\text{M}^{2+}$ has been observed to be possible. Regarding the bandgap value, in materials composed by In-Cd-S T5 clusters the topology does not seem to influence the value of this parameter, since the materials obtained by Su et al. [62] and Wu et al. [64] have the same bandgap value, although the first is a layered material and the second isolated clusters.

Some years after the synthesis of a true T5 cluster, a T6 cluster was obtained [66]. In order to achieve a cluster of that size without adding organic ligands to stabilise the negative charges, a mixed metal strategy is used, in order to have some high valence cations at the corners of the cluster that allow to reduce the global charge. In order to achieve that, the ratio $\text{M}^{2+}/\text{M}^{3+}$ of an ideal T6 cluster should be 1. In the T6 cluster obtained, named OCF-100, all Zn ions are located at the core or at the faces of the cluster and the edges are occupied by In^{3+} .

3.2 Super-supertetrahedral Clusters $\text{T}_{p,q}$

It was observed that in some cases four T_n clusters were organised in a polyhedra structure, giving rise to a supertetrahedron, called $\text{T}_{p,q}$, which means that T_p clusters are organised in a T_q cluster using a X^{2-} as a linkage between the clusters [67].

The first time such structure was obtained was by Li et al. [68]. The synthesised structure consists of the presence of T2 clusters organised in a T4 cluster, thus leading to the presence of $\text{T}_{2,4}$ units with the composition $\text{Cd}_{16}\text{In}_{64}\text{S}_{134}$. When an ionic exchange was performed in order to attempt to substitute the organic counterions with inorganic cations no exchange was observed, showing how strong the ionic forces between the organic agent and the crystal are.

Continuing the work to obtain structures based on this type of clusters, Wang et al. [67] obtained a structure based on the infinite arrangement of T5 clusters, i.e. that presents a structure based on $\text{T}_{5,\infty}$. The material obtained, entitled CIS-11, is an example of the super supertetrahedral arrangement for the Cu-In-S chemical system. In order to obtain the $\text{T}_{5,\infty}$ arrangement it is observed that the corner sulphur atom has a coordination 4, responsible for connecting 4 T5 clusters, being the first time such connection between clusters is observed. Some years later it was obtained another structure, entitled CIS-27, also based on the arrangement of T5 clusters into a $\text{T}_{5,\infty}$ crystal [69]. CIS-27 presents a different connection mode between the different T5 clusters when compared to CIS-11. For each group of 4 T5 clusters, three are connected through a 3-coordinated sulphur atom and the remaining T5 cluster is connected to just one cluster. A material was then obtained, entitled ITF-9, based on the T4 In-Zn-S clusters which were geometrically arranged to form a $\text{T}_{4,\infty}$ crystal [70]. ITF-9 presents a single-diamond topology and after an ionic exchange with Cs^+ to eliminate the template molecules the structure

maintains its crystallinity. The stability of ITF-9 was also compared with UCR-1 and UCR-8. UCR-1 and UCR-8 also consist of T4 clusters, but the mode of connection between the clusters is different. In UCR-1 the clusters are connected through a bicoordinated sulphur bridge and in UCR-8 the clusters are connected through a tricoordinated sulphur bridge. Although the ITF-9 maintains its diffraction pattern after the ion exchange at room temperature, the intensity of the peaks associated with the UCR-1 and UCR-8 structures decrease drastically. When the ion exchange is performed at a higher temperature, ITF-9 is able to maintain its structure. The same is not true for UCR-1 and UCR-8, with the collapse of the structures.

3.3 Pentasupertetrahedral Clusters Pn

Another example of tetrahedral clusters are the penta-supertetrahedral clusters Pn . Each Pn cluster can be seen as an assembly of four Tn tetrahedrally distributed into the four faces of one anti- Tn cluster. An anti- Tn cluster is a Tn cluster where the positions of cations and anions are exchanged. $P1$ and $P2$ clusters can be found as building blocks in a wide variety of open frameworks. Comparing to a Tn cluster of the same order, a Pn cluster has larger dimensions. For that reason, it is harder to prepare materials that uses Pn clusters as building units [23] [38] [71]. The number of cations in a Pn cluster is given by $t_n = [4n(n+1)(n+2)/6] + [(n+1)(n+2)(n+3)/6]$ and the number of anions is given by $x_n = [4(n+1)(n+2)(n+3)/6] + [n(n+1)(n+2)/6]$.

A $P1$ cluster consist of four $T1$ MX_4 clusters and one anti- $T1$ XM_4 at the core, resulting in a $P1$ cluster with the composition M_8X_{17} [71]. Zimmermann et al. [72] and Dehnen et al. [73] obtained $P1$ clusters of the type $M_4Sn_4Se_{17}$ ($M = Zn, Mn, Co$). A 3D structure was then obtained based on the $Cd_4Sn_3Se_{13}$ cluster, which derives from $Cd_4Sn_4Se_{17}$, originating a polar open-framework [74]. The extra framework is occupied by K^+ cations which can be exchanged with other cations such as Li^+ , Na^+ or Rb^+ , while maintaining the structure of the material.

Continuing the research to obtain $P1$ clusters, Palchik et al. [75] obtained clusters based on sulphur instead of selenium, presenting the chemical formula $M_4Sn_4S_{17}$ ($M = Zn, Mn, Co, Fe$). Also based on the $Zn_4Sn_4S_{17}$ cluster, Manos et al. [76] [77] obtained a 3D structure. To form the 3D framework each cluster is connected to four Sn atoms through the four terminal sulphur atoms. In turn, each Sn atom is connected to four clusters. The connection of clusters through metal centers is somewhat rare when it comes to methods of connection between clusters. Regarding the topology of the structure, it is of the diamond type with three different sizes of cavities. Each cavity has a distinct chemical reactivity, since the distribution of K^+ cations is different in each cavity. Due to the difference in cavity chemical reactivity, the structure has a high Cs^+ selectivity, even in the presence of large excess of Li^+ , Na^+ , K^+ or Rb^+ . In the absence of Cs^+ , the structure has a high ion-exchange capacity for NH_4^+ , comparable to that of natural zeolites.

As for 3D structures based only on $P2$ clusters (see figure 6), Lv et al. [78] were able to synthesise such structures, entitled it MCOF-1 and MCOF-2. Both materials are based on a combination of Sn-In-Cu. MCOF-2 presents an interrupted open framework, which is somewhat rare for these of type of structures. As for the topology, MCOF-1 has a chiral srs and MCOF-2

a double diamond. Although MCOF-1 and MCOF-2 have different topologies, the band-gap values are similar. Both structures collapse after an ion exchange with Cs^+ .



Figure 6: P2 cluster composed by T2 and anti-T2 cluster [78]

As can be seen, most of the structures obtained are molecular, and there is no example of a laminar structure composed by this type of clusters.

3.4 Capped Supertetrahedral Clusters C_n

A third example of tetrahedral clusters is the Capped Supertetrahedral series C_n . Each C_n cluster consists of a T_n cluster covered by a shell of atoms. Each face of the T_n cluster is covered by the bottom atomic sheet of a $T(n+1)$ cluster and each corner covered by a metal-chalcogenide group. Thus, the stoichiometry of a M_xX_y type C_n cluster is equal to $x = [n(n+1)(n+2)]/6[4(n+1)(n+2)]/2+4$ and $y = [(n+1)(n+2)(n+3)]/6+[4(n+2)(n+3)]/2+4$ [23].

Lee et al. [79] obtained for the first time a $C1$ cluster with the composition $\text{S}_4\text{Cd}_{17}(\text{SPh})_{28}$. Later, a 3D structure based on the $C1$ $\text{Cd}_{17}\text{S}_4(\text{SCH}_2\text{CH}_2\text{OH})_{26}$ cluster [80] and a 3D polymeric complex based on $[\text{S}_4\text{Cd}_{17}(\text{SPh})_{24}(\text{CH}_3\text{OCS}_2)_{4/2}]_n \cdot n \text{CH}_3\text{OH}$ [81] were also synthesised.

The first material based on $C2$ cluster, with the composition $\text{Cd}_{32}\text{S}_{14}(\text{SC}_6\text{H}_5)_{36} \cdot \text{DMF}_4$, was obtained by Herron et al. [82]. Vossmeier et al. [83] obtained a similar structure but with different organic residues. It was observed that the organic residue has a direct influence on the final architecture as well as on its optical properties of the final material. Other examples of materials based on the $C2$ cluster can be found in the literature. For example, Behrens et al. [84] obtain an unusual $C2$ cluster based on Hg-Se chemical system where the Hg atoms adopt an almost trigonal planar coordination, and Eichhöfer et al. [85] synthesised the first manganese chalcogenide $C2$ clusters.

Within this series of clusters, another similar one appears, entitled C_n, m . A C_n, m cluster has the same chemical composition as a C_n cluster, but has a different spatial arrangement of the corner atomic unit. The C_n, m cluster is obtained by rotating one of the atomic units 60° . Each C_n cluster has 4 atomic units and each one can be rotated independently, giving rise to four distinct series (m corresponds to the number of atomic units rotated) [23].

Zheng et al. [86] obtained the first example of clusters of this series. The cluster $\text{Cd}_{54}\text{S}_{32}(\text{SPh})_{48}(\text{H}_2\text{O})_4$ is the first example of C3,4 and $\text{Cd}_{32}\text{S}_{14}(\text{SPh})_{40}$ the first example of C2,2. It was also observed that it is possible to dope the C3,4 clusters obtained with Fe or Co.

It can therefore be concluded that clusters of this series have not yet been obtained without the presence of an organic component and that the materials obtained are only the result of the combination $\text{M}^{2+}\text{-X}$ ($\text{X} = \text{S}, \text{Se}$).

3.5 Oxyclusters

Metal chalcogenides may present stability problems, namely when used as photocatalysts. Therefore, it is expected that the formation of oxycluster-based structures will have a superior stability, being able to maintain the electronic properties, such as suitable band structures and favourable absorption in the visible region, of metal chalcogenides [87].

The first isolated $\text{Sn}_{10}\text{O}_4\text{S}_{20}^{8-}$ oxycluster was obtained in 1975 by Schiwy et al. [88]. Kaib et al. [89] obtained the same isolated anion but instead of the counterpart being Cs as before, Li was used as a counter cation. Due to the replacement of Cs by Li, the water present is about 2,5 times higher than that of the structure with Cs.

Parise et al. [90] obtained for the first time a 3D structure with a 4-connected porous system using as building units the clusters previously obtained by Schiwy et al. [88]. The material obtained, titled TETN-SnOS-SB2, presents a two-interpenetrating network and a topology analogous to cristobalite. Continuing the research to obtain structures based on the T3 $\text{Sn}_{10}\text{O}_4\text{S}_{20}^{8-}$ cluster, the same research team obtained a layered material, entitled TMA-SnOS-SB3 [91]. It was observed that it is possible to obtain the TETN-SnOS-SB2 or TMA-SnOS-SB3 structures from the analogous non-oxygen frameworks. Although the source of oxygen is not known, one possible hypothesis for the origin of this element is the decomposition of the water used as a solvent in the gel.

Huang et al. [92] obtained for the first time a material composed of T4 $\text{Sn}_{20}\text{O}_{10}\text{S}_{34}$ oxyclusters. Such material presents a two-fold interpenetrating diamond framework and maintains its structure in an environment with a pH from 1 to 13 for a period of one week. When an attempt was made to eliminate the organic compounds present in the porous system by ion exchange with Cs^+ , it was observed that the porosity of the sample did not change. Regarding the In-O-S chemical system, Zhang et al. [93] obtained a three-dimensional material based on the pseudo T4 $\text{In}_4\text{Sn}_{16}\text{O}_{10}\text{S}_{34}$ cluster for the capture of heavy metals. Regarding topology, this material presents a two-fold interpenetrated framework analogue to cristobalite. Continuing research to obtain materials based on large clusters, Yang et al. [94] were able to obtain for the first time T5 oxycluster-based materials made by the combination of In, O and S chemical elements.

Zhang et al. [95], in order to develop a catalyst for oxygen reduction reaction, obtained isolated Ge-Zn P1 oxyclusters doped by Mn. The clusters obtained are more stable than the traditional P1, due to the replacement of S^{2-} with OH⁻ at the four corners of the cluster.

As for the Ga-S-O system, Vaqueiro et al. [49] were successful in obtaining a 3D structure based on a T3 cluster where the terminal sulphur was substituted by an oxygen atom. The connection between the clusters is made by an unusual polysulphide linkage and it is the first

time that the linkage of these types of clusters is made through a O^{2-} bridge.

Aharia et al. [96] studied the Sn-Se chemical system. It was observed that there is a change of phases between a $TMA_2Sn_3Se_7$ laminar material to a $TMA_2Sn_5Se_{10}O$ three-dimensional material. What differentiates the achievement of the different phases are the number of days and the temperature of synthesis. It was observed that for two days of synthesis, a laminar monocyclic phase is the only phase present. On the fourth day of synthesis, three distinct phases coexist: two laminar orthorhombic and monocyclic phases and a third unknown phase. On the seventh day of synthesis there is a fourth phase associated with a three-dimensional tetragonal material which becomes the only phase present after 16 days of synthesis. The three-dimensional material consists of T2 $Sn_4Se_{10}O$ clusters with the oxygen atom located in the centre. Continuing the research in obtaining selenium-based materials, Lin et al. [87] obtained a material based on the T3 $Sn_{10}O_4Se_{20}$ cluster. The structure obtained, entitled OCF-61-SnOSe, can be deconstructed into three levels of organisation. The primary building unit is the $SnSe_4$ tetrahedron. The next structural level would be to obtain a T3 $Sn_{10}Se_{20}$. However, its formation is unfavourable, as it is an unstable structure due to the excessively high bond valence due to Sn^{4+} . Thus, a T3 $Sn_{10}O_4Se_{20}$ is formed, where four adamantane-type cages surround a O^{2-} , being the secondary building unit. The tertiary building unit is the formation of the super-supertetrahedral cluster. Four T3 $Sn_{10}O_4Se_{20}$ are connected through bicoordinated Se^{2-} but also through a dimeric $Sn_2Se_6^{4-}$, originating a T2 cluster. Therefore, OCF-61-SnOSe can be characterised by the presence of the super-supertetrahedral $T_{3,2}$ cluster which presents a honeycomb layered structure.

3.6 TOn series

TOn differs from *Tn*, *Cn* to *Pn* cluster series so far presented, as they result from the combination of tetrahedral and octahedral bonding features in the same cluster. Such clusters result in the combination of a NaCl-like octahedral core covered by a ZnS -like tetrahedral shell.

The first example of a structure based on this type of clusters was obtained by Wu et al. [97]. This structure, entitled OCF-41, is made up of In-S TO2 clusters. The TO2 cluster consists of an $In_{10}S_{13}$ octahedral core which presents on the corners four T2 In_4S_{10} clusters and on the faces four hexagonal In_3S_3 rings (see figure 7). OCF-41 presents a two-dimensional structure where the TO2 clusters are connected through dimeric $In_2S(H_2O)_2$ units.

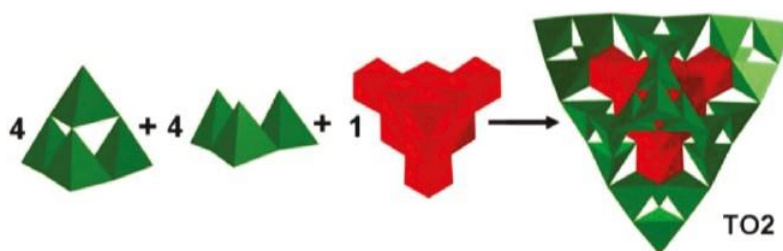


Figure 7: TO2 cluster composed by four T2 clusters, four hexagonal rings and an octahedral core [97]

Due to the high negative charge associated with the TO₂ cluster it is difficult to counter-balance it using the usual templates, thus limiting the construction of structures with high dimensions. One of the methodologies used by Wang et al. [98] to obtain a three-dimensional structure using TO₂ clusters as building units was through the introduction of high-valence metal cations. Two 3D structures, entitled SOF-25 and SOF-28, based on In-Sn-S TO₂ clusters were obtained. SOF-25 presents a double interpenetrated diamond framework and SOF-28 a triple interpenetrated diamond framework.

3.7 Structures with different series and types of clusters

Examples of structures consisting of only one type of cluster as a building unit were presented. However, it is possible to have materials composed by more than one type of cluster. Thus, by increasing the complexity and diversity of these systems, it is possible to synthesise materials with physical and chemical characteristics adapted to a specific application.

Starting with the T n clusters, there are 4 types of clusters, thus it is possible to have 6 different combinations: T2-T3, T2-T4, T2-T5, T3-T4, T3-T5 and T4-T5. The biggest challenge of synthesising structures based on different T n clusters is the phase separation, ending with two distinct structures containing only one type of cluster.

Han et al. [99] synthesised for the first time a compound that consisted on the presence of Sn-Ga-S T2 cluster and the uncommon Sn-S-O T3 cluster, adopting a PtS type topology.

The first example of a T2-T4 combination is presented by Wu et al. [59]. The synthesised structure, OCF-42, results in a combination of M⁴⁺/Ga³⁺/Se²⁻ T2 cluster and Ga³⁺/Zn²⁺/Se²⁻ T4 cluster. The structure is not constituted through the alternation of the two types of clusters. Each T2 cluster is connected to four T4 clusters and each T4 cluster is connected to one T2 cluster and three T4 clusters, thus obtaining a T2/T4 framework ratio equal to 1:4. The structures obtained have a band gap approximately equal to 1.5 eV.

As for the T2-T5 combination, Wang et al. [100] managed to obtain such structure, entitled CIS-52, through the combination of Ge-In-Cu-S. The starting system was In-S and the addition of Cu favours the formation of T5 clusters while the presence of Ge favours the formation of T2 clusters. In this case, the structure is composed through the alternation of clusters.

When Zheng et al. [41] obtained for the first time a structure based on the Ga-Zn-S T4 cluster system, it was also observed that by changing the structuring agent, a structure based on the alternation of clusters type T3 and T4 is obtained, the UCR-19 structure. Another example of a structure based on the presence of T3 and T4 clusters is presented in [49], being the first example of the incorporation of Co on the Ga-S system.

The 3D structure synthesised by Wang et al. [61] where, for the first time a pseudo-T5 cluster was obtained, is based on the alternation of the pseudo T5 cluster with T3 clusters. Another example of a 3D structure composed by the combination T3-T5 clusters is the material obtained by Zhang et al. [101], named IOS-35. In such material the T3 clusters are composed by In and S and the T5 clusters are oxyclusters, presenting a combination of In, O and S.

A material with the combination T4-coreless T5 was first obtained by Wang et al. [102]. Such structure, entitled OCF-45, presents a non-interpenetrated diamond topology and it is

based on the In-Mn-S chemical system. OCF-45 presents an large extra framework volume and windows aperture due to the non interpenetrating topology and the presence of big clusters size. For the elimination of the structure directing agents, a simple ion exchange with Cs^+ can be done to perform such elimination. However, a small shift of the diffraction peaks towards lower angles can be observed, since with the elimination of the large organic species the crystalline framework tends to shrink.

As for structures based on different clusters, Zhang et al. [103] manage to synthesise a material, entitled HCF-1, which was composed by P1 and T2 clusters of the chemical system In-S, presenting a 2D framework. Following these works, a 3D structure based on $\text{T}_{3,2}$ and T_3 clusters from the Sn-In-S chemical system was obtained [104]. In such structure, entitled SOF-2, each $\text{T}_{3,2}$ clusters is connected to four T_3 clusters.

Of all the observed combinations, it should be noted that no material has yet been obtained that results from the combination of M^{4+} and M^{2+} metals.

4 Non Tetrahedral Clusters

Due to the tetrahedral coordination of Tn , Pn and Cn clusters series, these units become the ideal candidates for the construction of open frameworks. However, the number of clusters available is limited. Moreover, clusters in the Pn and Cn series tend to maintain their isolated form rather than forming open frameworks. It is therefore desirable to create other series of clusters in order to enrich the cluster-based chalcogenide open frameworks [98].

4.1 Semi-cube Clusters

Regarding this type of clusters, two possible compositions stand out: Sb_3S_6 and Sn_3S_4 [24].

Parise et al. [105] obtained for the first time a layered material based on the Sb_3S_6 cluster. When tetramethylammonium ion is used as a template, a three-dimensional structure is obtained [106]. Research continued into this chemical system, using large tertiary amines in order to try to produce materials with larger cavities [107]. When tetrapropylammonium hydroxide or triethylenetetramine is used, no three-dimensional materials are obtained, but 1D and 2D structures, respectively.

The materials obtained by Bedard et al. [26] [27] in 1989 are the first examples of layered materials composed by the semicube Sn_3S_4 clusters. Next, Jiang et al. [108] [109] [110] [111] [112] have studied the Sn-S system, obtaining layered materials based on the periodic arrangement of Sn_3S_4 clusters. Two types of layered materials were obtained: SnS-1 and SnS-3. The difference between the two is based on the way the clusters are connected. SnS-1 presents a hexagonally shaped 24-atom rings and SnS-3 has a elliptically shaped 32-atom rings. It has been observed that when using small size templates, such as tetrabutylammonium hydroxide, SnS-1 is obtained and large size templates, for example tetrapropylammonium or tetrabutylammonium hydroxides, originate SnS-3. Both structures have a surprising flexibility. In order to accommodate templates with different shapes or dimensions, the synthesised materials may undergo a certain elastic deformation, changing the interlamellar spacings instead of forming a

structure with a new topology. Another important characteristic of these materials is their thermal stability when removing the template used during their synthesis. SnS-1 was also subjected to an ion-exchange study. When tetramethylammonium hydroxide is located in the intralaminar space, it is possible to exchange part of the organic component with Na^+ , Ca^{2+} , Co^{2+} or Ni^{2+} . When trying to exchange with Cu^{2+} or Ag^+ , the structure collapses [113]. Bowes et al. [114] performed a more in-depth study of the SnS-1 structure. It was noted that it is possible to use tetramethylammonium (TMA), tert-butylammonium (TBA) or quinuclidinium (QUIN) as organic template to obtain the structure. Such species occupy the interlaminar space, being responsible for counterbalancing the charge of the framework, but also to support it. The size and shape of the template is responsible for controlling the interlaminar distance, but also the thermal stability and adsorption and sieving properties of the material. The SnS-1 structure is able, to a certain extent, to exchange with other species, occurring swelling of the structure. When the species are too large, they are simply excluded, thus having a sieving effect. The substitution of sulphur by selenium was also evaluated. The analysis of diffraction data allows to state that the structures of the materials $\text{TMA}_2\text{Sn}_3\text{S}_7$ and $\text{TMA}_2\text{Sn}_3\text{Se}_7$ are identical. However, an increase in lattice was observed due to the larger size of the Selenium than the Sulphur. It is also possible to obtain the SnS-1 structure from tris-2-aminoethylamine [115] [116] or 1-(2-aminoethyl)piperidine [116], thus showing the flexibility of this structure to accommodate different molecules into their interlayer space. Qi et al. [117] continued to study the ion-exchange properties of SnS-1. After exchanging with Cs^+ or Sr^{2+} , the material maintains its crystalline structure, and there is a reduction in the material's band gap. Filso et al. [116] also observed that the component occupying the interlaminar space has a direct effect on the band gap of the material.

Switching to selenium-based materials, Han et al. [118] obtained 1D and 2D materials with the Sn_3Se_4 semicube cluster, using the alcohol $\text{C}_2\text{H}_5\text{OH}$ as a solvent. The laminar material has a honeycomb structure with elliptical holes with $\text{Mn}(\text{en})_3^{2+}$ cations at the nanochannels. For the 1D structure, it can be seen as an anionic zig-zag chain with $\text{Ni}(\text{en})_3^{2+}$ located between the chains.

4.2 Icosahedral Clusters

As seen above, the presence of monocations such as Cu^+ [33] [34] [35] or Ag^+ [35] is restricted to connecting the clusters or to partially replacing the cationic sites of the tetrahedral clusters. With the increase in the content of monocations in the framework, new clusters emerge, where the icosahedral clusters stand out. This type of clusters has 6 connection modes, allowing to obtain topologies that would not be possible to obtain with tetrahedron clusters. To obtain this type of icosahedral clusters the presence of high valence cations with a tetrahedral coordination is essential, since it reduces the negative charge of the chalcogenide ions [119]. The monocation that has been the subject of most research is copper, originating a new family of materials entitled copper-rich open-framework chalcogenides. Due to the high copper content in the structures, there is a red shift in the band gap, making these materials promising when it comes to applications in the areas of photovoltaic and photocatalysis applications [120].

The first examples of structures with icosahedral cluster as building units were obtained by Schimek et al. [121]. The three-dimensional structure obtained consists of the connection of Cu_8S_{13} icosahedral clusters through Sb atoms that assume a tetrahedral coordination with the sulphur atoms.

Following these works, Zhang et al. [122] obtained a material based on icosahedral clusters composed by Cu and S using Ge as a connection mode. Regarding the structure, it can be seen as a cubic packing of Cu_8S_{12} icosahedral clusters that are connected in two directions by dimeric Ge_2S_6 units and on the other direction by GeS_4 . Comparing with three-dimensional structures composed by T2 clusters with the same chemical elements, it can be observed that the structure formed by icosahedral clusters presents a higher number of Cu than Ge, thus contributing to the low value of the band gap and the photocatalytic activity in the visible region of the material. Continuing the research on this series of materials, it was possible to obtain structures also composed by Cu_8S_{12} icosahedral clusters that were only connected by GeS_4 units [123]. The structures obtained present the 3D topology of perovskite. Comparing the two structures, the structure that only presents as GeS_4 units as a link between the clusters needs only K^+ or Rb^+ instead of organic amines to stabilise the structure. A structure composed by Cu_8S_{12} icosahedral clusters connected in two directions through GeS_4 and in one direction by Ge_2S_6 dimeric unit was then obtained [124]. Comparing the three materials, the one that presents the biggest extra framework volume is the material obtained in [122], followed by [124] and the one with smaller extra framework volume is [123]. This can be explained by the way clusters are connected: the more connections are made by Ge_2S_6 dimeric units, the more the framework will expand.

More recently, Tang et al. [125] have obtained a 3D structure composed of Cu_8S_{12} icosahedral clusters that are surrounded by Cu_8S_{16} rings. Such structure presents GeS_4 tetrahedra entrapped, being the first time tetrahedrons have not participated in the cluster connection.

It is possible to find in the literature materials that use Sn^{4+} instead of Ge^{4+} to connect the different clusters [126] [127]. Due to the way the different clusters are connected, the material obtained by Zhang et al. [126] presents a multiple channel system, something rare for a material with a cubic symmetry. Behrens et al. [127] also obtained a series of materials based on Cu_8S_{12} icosahedral clusters. In some materials obtained it was observed for the first time the inclusion of Sn^{3+} in the cluster, being the first example of materials based on $\text{Cu}_7\text{SnS}_{12}$ icosahedral clusters while still using Sn^{4+} as a connection between the clusters.

For seleniums, the first series of 3D materials were obtained by Zhang et. al [119]. This series of materials are based on the presence of $\text{Cu}_8\text{Se}_{13}$ icosahedral clusters that are connected by AsSe_3 tetrahedral units. Yang et al. [128] then obtained a three-dimensional framework based on the presence of $\text{Cu}_8\text{Se}_{13}$ icosahedral and Cu_4Se_6 octahedral clusters. Each icosahedron is connected to six tetrahedrons through six distorted SnSe_4 and each tetrahedron is connected to three icosahedrons through three SnSe_4 via sharing vertex and Se-Se bonds. Due to this method of connection, the material obtained presents (3,6)-connected pyr topology. When trying to eliminate the organic component via ion exchange with Cs^+ or Na^+ , it is not successful. Luo et al. [120] were able to obtain for the first time a family of materials where the icosahedral clusters were connected only by Ge_2Se_6 or Sn_2Se_6 dimers. This was achieved by using templates

with low charge density. As the only method of connection is via dimer, this family of materials has the highest extra framework volume. It was also obtained for the first time a material composed by $\text{Cu}_7\text{GeSe}_{13}$ clusters. Such materials have the PCU topology, analogue to the topology of MOF-5. The band gap of structures composed of Cu-Sn-Se and Cu-Ge-Se was also compared and it was concluded that the structures composed of Cu-Sn-Se present a narrower band gap than those composed by Cu-Ge-Se. Another examples of 3D material consisting of Ge-Cu-Se are the materials obtained by Wang et al. [129]. The framework of the first material consists of two types of clusters, $\text{Cu}_8\text{Se}_{13}$ icosahedral and Cu_4Se_6 octahedral, that are connected through bridging with $\text{GeSe}_3(\text{Se}_2)$ units. Such connection mode between the clusters originates a material with a pyr topology. The second material can be seen as a 3D framework composed by $\text{Cu}_8\text{Se}_{13}$ connected solely by Ge_2Se_6 dimers.

5 Zeolite Analogue Structures

Zeolites are an important family of microporous crystalline inorganic materials, with numerous applications in the petrochemical industry as catalysts. Zeolites present the general formula $A_{x/n}[\text{Si}_{1-x}\text{Al}_x\text{O}_2] \cdot m \text{H}_2\text{O}$, where A is a metal cation with a valence n . Regarding their structure, the more than 100 different architectures known are based on the connection through the vertices of the tetrahedrons TO_4 , where T, the T atom, can be Si or Al. It is possible to find numerous porous materials based on zeolites, where the T atom is replaced by other elements, such as Ga, Ge or P [130]. However, these materials, because they are oxide-based, are insulating and therefore have limited applications in photo, electro and optical fields. In recent years, chalcogenide-based semiconductor zeolites has been synthesised, where the oxygen is replaced by another chalcogen (such S, Se or Te), and the T atom by another metallic cation tetracoordinated. This strategy has been successful in obtaining semiconductor structures with high surface area. However, the number of structures with the IZA structure code remains small. Although there are many 3D microporous chalcogenide structures, as noted earlier, the presence of different anion coordination and the possible absence of tetravalent metal ions leads to the creation of non-zeolite structures [131]. As the size of the cluster increases, some characteristics that make the structure non-zeolite appear, such as anions with 3 or 4 coordination. Thus, the structures analogous to zeolites are generally based on T2 clusters, where metallic ions with high valence are used to balance the overall charge of the structure [132].

The first reference to a material with an analogue structure to a zeolite is from 1997. The material obtained by Cahil et. al [133] consists on the presence of T2 Ge_4S_{10} clusters that are connected by Mn. Using 1,4-diazabicyclo[2.2.2]-octane as template it is possible to obtain an analogous structure to Li-A(BW) zeolite where the SiO_4 and AlO_4 were substituted by MnS_4 and Ge_4S_{10} , respectively.

Zheng et al. [16] obtained a series of zeolite analogous materials based on the combination of M^{4+} and M^{3+} in the same cluster. In order to synthesise clusters involving both cations and to avoid the formation of two types of clusters consisting only of M^{4+} or M^{3+} , Zheng et al. resorted to a synthesis in a non-aqueous medium in order to overcome such problem. The

zeolite analogues materials obtained were design through a triple replacement of O^{2-} by S^{2-} or Se^{2-} , Si^{4+} by Ge^{4+} or Sn^{4+} , and Al^{3+} with Ga^{3+} or In^{3+} . Any M^{4+}/M^{3+} combination is possible. Due to the different possible combinations, it is feasible to customise the physical properties of the final material, such as band gap, luminescence, pore size, surface area, ion exchange and chemical stability. The previously synthesised 3D structures generally have a low thermal stability, collapsing at temperatures below $300^{\circ}C$. In order to avoid such a situation, the M^{4+}/M^{3+} ratio should preferably be between 0,2 and 1,2. This is contrary to the rule of stability of zeolites, which states that the M^{4+}/M^{3+} ratio should not be less than 1. The different synthesised samples were grouped into 4 families: UCR-20, UCR-21, UCR-22 and UCR-23. Each family refers to materials with the same framework topology but different chemical compositions. UCR-20, UCR-21 and UCR-23 have as building units T2 type clusters while UCR-22 presents a coreless pseudo-T4 cluster as building unit. Regarding topology, UCR-20 presents the sodalite framework, UCR-21 has a diamond structure, UCR-22 has two interpenetrating diamond structure and UCR-23 has a CrB_4 type topology. These materials have an extra large pore. UCR-20 and UCR-21 have a large pore size, consisting of 12 T atoms, while UCR-22 and UCR-23 have an extra large pore size, consisting of 24 and 16 T atoms respectively. The main characteristics of the different materials obtained are systematised in the table 5. As for the elimination of the template, it was possible to perform a calcination at 350° under a N_2 atmosphere without destroying the structure of UCR-20-GaGeS-TAEA. It was also observed that an ion exchange with CsCl is also able to eliminate the template.

Table 5: Different zeolite analogue materials obtained by Zheng et al. [16] and their chemical composition, final topology and pore size

Material	Template	Composition			Cluster	Structure	Pore Size
		M ⁴⁺	M ³⁺	X ²⁻			
UCR-20-GaGeS-TAEA	TAEA ¹	Ge	Ga	S	Ga ₁ · ₈ Ge ₁ · ₃₃ S ₈	3D - SOD ²	12 T Atoms
UCR-20-GaSnS-TMDP	TMDP ³	Sn	Ga	S	Ga ₁ · ₈ Sn ₂ · ₂₃ S ₈	3D - SOD ²	12 T Atoms
UCR-20-InGeS-TMDP	TMDP ³	Ge	In	S	In ₃ Ge ₁ S ₈	3D - SOD ²	12 T Atoms
UCR-20-InSnS-TMDP	TMDP ³	Sn	In	S	In ₂ · ₅ Sn ₁ · ₅ S ₈	3D - SOD ²	12 T Atoms
UCR-20-GaGeSe-TMDP	TMDP ³	Ge	Ga	Se	Ga _x Ge ₄ XSe ₈	3D - SOD ²	12 T Atoms
UCR-21-GaGeS-APO	APO ⁴	Ge	Ga	S	Ga ₃ · ₃₀ Ge ₀ · ₇₀ S ₈	3D - D ⁵	12 T Atoms
UCR-21-GaSnS-TAEA	TAEA ⁶	Sn	Ga	S	Ga ₂ · ₃₂ Sn ₁ · ₆₈ S ₈	3D - D ⁵	12 T Atoms
UCR-21-InGeS-APP	APP ⁷	Ge	In	S	In ₁ · ₈₄ Ge ₂ · ₁₆ S ₈	3D - D ⁵	12 T Atoms
UCR-21-InSnS-AEP	AEP ⁸	Sn	In	S	In _x Sn ₄ xS ₈	3D - D ⁵	12 T Atoms
UCR-21-GaSnSe-TAEA	TAEA ⁶	Sn	Ga	Se	Ga ₂ · ₄₇ Sn ₁ · ₅₃ Se ₈	3D - D ⁵	12 T Atoms
UCR-22-GaGeS-AEP	AEP ⁸	Ge	Ga	S	Ga ₃ · ₃₃ Ge ₀ · ₆₇ S ₈	3D - DD ⁹	24 T Atoms
UCR-22-GaSnS-AEP	AEP ⁸	Sn	Ga	S	Ga ₂ · ₁₃ Sn ₁ · ₈₇ S ₈	3D - DD ⁹	24 T Atoms
UCR-22-InGeS-AEP	AEP ⁸	Ge	In	S	In ₂ · ₆₉ Ge ₁ · ₃₁ S ₈	3D - DD ⁹	24 T Atoms
UCR-22-GaSnSe-TOTDA	TOTDA ¹⁰	Sn	Ga	Se	Ga ₁ · ₇₃ Sn ₂ · ₂₇ Se ₈	3D - DD ⁹	24 T Atoms
UCR-23-GaGeS-AEM	AEM ¹¹	Ge	Ga	S	Ga ₂ · ₆₇ Ge ₁ · ₃₃ S ₈	3D - CrB ₄ ¹²	16 T Atoms
UCR-23-GaSnS-AEM	AEM ¹¹	Sn	Ga	S	Ga ₂ · ₂₉ Sn ₁ · ₇₁ S ₈	3D - CrB ₄ ¹²	16 T Atoms
UCR-23-InGeS-AEM	AEM ¹¹	Ge	In	S	In ₁ · ₈₄ Ge ₂ · ₁₆ S ₈	3D - CrB ₄ ¹²	16 T Atoms

¹Tris(2-aminoethyl)amine. ²Sodalite (see figure 2b). ³4,4'-trimethylenedipiperidine. ⁴dl-1-amino-2-propanol. ⁵Diamond (see figure 3).

⁶Tris(2-aminoethyl)amine. ⁷1-(3-aminopropyl)-2-pipecoline. ⁸1-(2-aminoethyl)piperazine. ⁹Double Diamond (see figure 2a).

¹⁰4,7,10-trioxa-1,13-tridecanediamine. ¹¹N-(2-aminoethyl)morpholine. ¹²Cristobalite (see figure 2c).

Lin et al. [134] have managed to synthesize structures rich in Ge or Sn, thus managing to obtain truly high silica zeolite analogous structures. It was observed that a small portion of divalent cations induce crystallisation of Sn/Ge rich structures. Four different topologies, CPM-120, CPM-121, CPM-122 and CPM-123, were obtained, although all the materials have as building units T2 clusters. The clusters of CPM-120 are organised to form the sodalite topology, obtaining the zeolite-type RWY framework. CPM-121 presents a non-interpenetrated diamond framework. Regarding CPM-122, it has a doubly-diamond framework. Finally, CPM-123 has a CrB₄ type structure, the same as the zeolite framework code BCT.

Table 6: Different zeolite analogue materials obtained by Lin et al. [134] and their chemical composition and final topology

Material	Template	Composition			Cluster	Structure
		M ⁴⁺	M ³⁺	X ²⁻		
CPM-120-ZnGeS	AEM ¹	Ge	Zn	S	Zn _{0.81} Ge _{3.19} S ₈	3D - SOD ²
CPM-121-ZnGeS	AEM ¹ , TBA ³	Ge	Zn	S	Zn _{0.93} Ge _{3.07} S ₈	3D - D ⁴
CPM-122-ZnCdGeS	AEM ¹ , LTD ⁵ , DBU ⁶	Ge	Zn, Cd	S	Zn _{0.65} Cd _{0.41} Ge _{2.95} S ₈	3D - DD ⁷
CPM-123-ZnGeS	AEM ¹ , HA ⁸	Ge	Zn	S	Zn _{1.21} Ge _{2.79} S ₈	3D - CrB ₄ ⁹
CPM-120-ZnSnSe	BPP ¹⁰	Sn	Zn	Se	Zn _{0.99} Sn _{3.01} Se ₈	3D - SOD ²
CPM-120-CdSnSe	BPP ¹⁰	Sn	Cd	Se	Cd _{0.68} Sn _{3.32} Se ₈	3D - SOD ²

¹N-(2-aminoethyl)morpholine. ²Sodalite (see figure 2b). ³Tributylamine. ⁴Diamond (see figure 3). ⁵2,6-Lutidine

⁶1,8-diazabicyclo[5.4.0]undec-7-ene. ⁷Double Diamond (see figure 2a). ⁸1-hexylamine. ⁹Cristobalite (see figure 2c).

¹⁰1,3-bis(4-piperidiny)propane.

After the synthesis, due to the blocking of the porous system by the structuring agents used, the samples show negligible gas adsorption. However, after exchange with Cs⁺, the synthesised materials show an isotherm type I. For thermal stability, e.g. CPM-120-ZnGeS sample maintains structural and mechanical integrity when heated in air at 310° for at least 1 hour, presenting itself as a thermally and chemically stable sample. Further studies have been conducted on the CPM-120-ZnGeS-AEM structure [135], namely on its charge selectivity. After performing an ionic exchange with Cs⁺, it was observed that the structure presents a selectivity towards cationic organic molecules, and can thus be used to respond selectively according to the charge properties of the compounds. It was also observed that this chalcogenide material presents, besides charge selectivity, size selectivity.

Wu et al. [136] were able to synthesise two zeolite analogues structures based on T2 clusters as building units, entitled SOF-20 and SOF-21, using a combination of In and Sn as the cations and a mixture of superbases as template. What differs these structures from those previously synthesised is the inter-cluster bridging angle. Generally, the values of this parameter are between 104° and 110°. The SOF-20 structure has a inter-cluster bridging angle between 107° and 128°, hence having the largest bridging angle observed for a 3D chalcogenide framework. SOF-21 also presents a surprisingly high inter-cluster bridging angle, between 106° and 113°. Looking now at the topology of the samples, the SOF-20 structure shows a non-interpenetrated gismondine net (see figure 8a), being the first time such topology is observed in this class of materials. Regarding SOF-21, it presents a twisted diamond topology (see figure 8b), having an extra framework volume slightly higher than the samples with a diamond topology of previously synthesised samples such as UCR-21 or CPM-121.



Figure 8: Representation of Gismondine (gis) and Twisted diamond (dia) topologies [136]

As for the porosity of the samples, although ion exchange with Cs^+ is generally used for the elimination of the structuring organic agents, this technique proved ineffective for the SOF-20 sample, since the structure collapses after the ion exchange procedure. As for the SOF-21 sample, it does not collapse after the ion exchange with Cs^+ . However, during the degassing process the structure collapse, thus not being possible to perform a gas adsorption experiment.

Lin et al. [131] synthesised a structure that presented ordered interrupted sites, allowing to precise doping the material and to help the creation of extra-large pores. The structure, entitled CSZ-5, is composed of tetracoordinated In and bicoordinated Se making up a T2 cluster with a new boracite-related topology. It is the first time that an interrupted network consisting exclusively of 3-MR has been observed. It is possible, due to the presence of interrupted sites, to dope the structure in order to adapt the electronic structure and the photoelectric characteristics of the material to a specific given application.

So far, zeolite-like structures are all made up of type T2 clusters and result from the combination of $\text{M}^{4+}/\text{M}^{3+}$ or $\text{M}^{4+}/\text{M}^{2+}$. Chen et al. [137] were able to synthesise a structure analogues to a zeolite based on the system $\text{M}^{4+}/\text{M}^{3+}/\text{M}^{2+}$ still using the T2 clusters as building units. Starting with the precursor gels previously used by Lin et al. [134], these were doped with Ga^{3+} , In^{3+} , Sn^{4+} or Cd^{2+} . Through progressive additions of Ga precursor into the gel it is observed that it helps to improve the morphology of the CPM-120 crystals. Regarding the location of Ga in the T2 cluster, it can occupy different positions, as it is shown that depending on the amount of Ga precursor added, it can substitute Ge or Zn. Ga will first substitute Ge and then it will replace Zn. For the addition of In, small quantities result in no uniform CPM-120 crystals being obtained. When the amount of In precursor increases, the formation of CPM-121 crystals is observed. After optimisation of the experimental conditions, it was possible to obtain the CPM-121 structure where Ge and Sn coexist in the same cluster. The same was observed after the addition of Cd: it is possible to obtain the structure CPM-121 where Zn and Cd coexist in the same cluster. The figure 9 shows the main experimental results obtained.

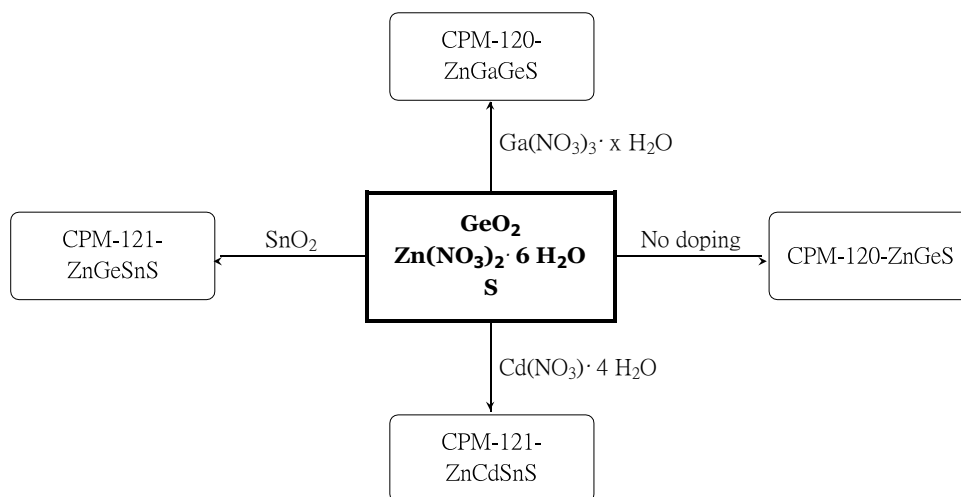


Figure 9: Schematic of the different forms of doping as well as the experimental results obtained in [137]

The doping studied has direct consequences on the optical properties of semi-conductors, as these depend heavily on the chemical composition of the materials. For example, when Ga replaces Ge, the value of the band gap increases. However, when Ga substitutes Zn, a decrease in the band gap is observed. The stability of the structures after ion exchange with Cs^+ was also studied. It was found that the CPM-120 structure is much more stable than the CPM-121 structure, with a thermal stability up to 610°C and a highly porous framework.

Xue et al. [132] obtained for the first time a zeolite analogous structures based on a combination of P1 and T2 clusters. The structures, entitled CSZ-9 and CSZ-10, are composed by In and S and present non interpenetrating frameworks based on C_3N_4 and SOD typologies, respectively. When an attempt was made to perform an ion exchange with Cs^+ to eliminate the organic structure agents, the structures collapsed. Later, the same team of researchers obtained two new structures based on the In-Se chemical system [54]. These structures, entitled CSZ-11 and CSZ-12, result in a combination of P1 clusters with defects. CSZ-11 and CSZ-12 present non interpenetrating frameworks and can be seen as extended crb and irl networks (see figure 10), respectively. In order to eliminate the organic template agents, a ionic exchange with Cs^+ was used. However, CSZ-11 collapses after the exchange and CSZ-12 collapses only after the degassing procedure necessary to do a N_2 adsorption measurements.

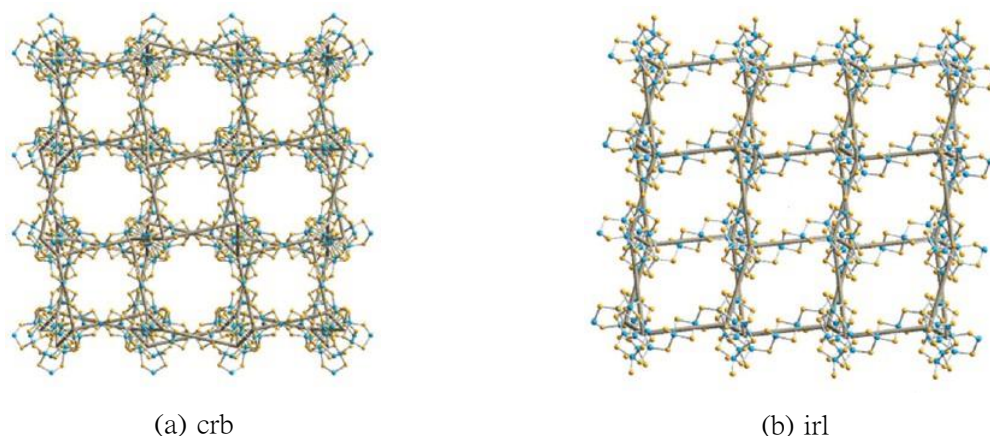


Figure 10: Representation of crb and irl topologies [54]

6 Hydrated Open Framework Chalcogenides

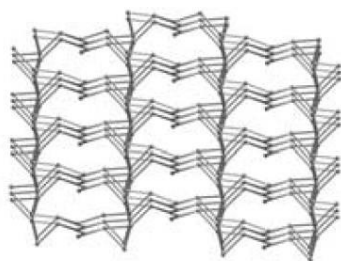
The majority of the layered or tridimensional materials previously presented were synthesised by hydro(solvo)thermal methods using structuring agents, which occupied an extra framework position. When a typical calcination is used to eliminate the organic component, most of the structures collapse. On some cases, those organic compounds could be exchanged with other inorganic cations, such as Cs^+ , without destroying the framework, thus releasing the porous volume of the structure. The synthesis of a system without the use of organic structuring agents is still subject of research, both for environmental and economic reasons.

However, only purely inorganic systems consisting of In^{3+} , $\text{In}^{3+}/\text{Cu}^+$ or $\text{In}^{3+}/\text{M}^{2+}$ ($\text{M}^{2+} = \text{Mn}$, Zn , Cd) are known [138]. All materials were synthesised in the presence of alkali or alkaline earth metal cations under highly alkaline conditions. The synthesis conditions used lead to the crystallisation of chalcogenides with encapsulated inorganic cations in their cavities. Seven different three-dimensional frameworks were synthesised and may present different chemical compositions: ICF-5, ICF-17, ICF-21, ICF-22, ICF-24, ICF-25 and ICF-27. A great diversity of clusters can be observed, as well as topologies of the different synthesised structures (see table 7).

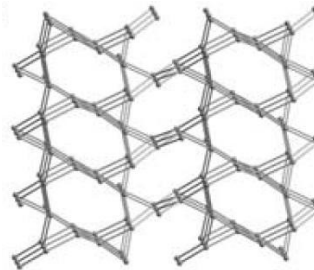
Table 7: Different materials obtained by Zheng et al. [138] and their chemical composition, final topology and pore size

Material	Composition				Cluster	Structure	Pore Size
	M ³⁺	M ²⁺	M ⁺	X ²⁻			
ICF-5-CuInS-Na	In	Cu	Na	S	T4 - Cu ₃ In ₁₇ S ₃₃	3D - DD ¹	-
ICF-5-CdInS-Na	In	Cd	Na	S	T4 - Cd ₄ In ₁₆ S ₃₃	3D - DD ¹	-
ICF-5-MnZnInS-Na	In	Mn, Zn	Na	S	T4 - Mn ₁ · ₈ Zn ₂ · ₂ In ₁₆ S ₃₃	3D - DD ¹	-
ICF-5-CdInS-Li	In	Cd	Li	S	T4 - Cd ₄ In ₁₆ S ₃₃	3D - DD ¹	-
ICF-5-ZnInS-Na	In	Zn	Na	S	T4 - Zn ₄ In ₁₆ S ₃₃	3D - DD ¹	-
ICF-5-MnInS-Li	In	Mn	Li	S	T4 - Mn ₄ In ₁₆ S ₃₃	3D - DD ¹	-
ICF-17-InZnS-Na	In	Zn	Na	S	T5 - In ₂₂ Zn ₁₃ S ₅₄	3D - DD ¹	-
ICF-21-InSe-Na	In	-	Na	Se	T2 - In ₄ Se ₈₄₂	3D - D ²	-
ICF-22-InS-Li	In	-	Li	S	pseudo T4 - In ₁₆ S ₃₂	3D - DD ¹	-
ICF-24-InSSe-Na	In	-	Na	S, Se	T2 - In ₄ S ₂ · ₉ Se ₅ · ₁	3D - ICF-24 ³	20 T Atoms
ICF-25-InS-SrCaLi	In	-	Sr, Ca, Li	S	T2 - In ₄ S ₈	3D - ICF-25 ⁴	16 T Atoms
ICF-27-InS-SrLi	In	-	Sr, Li	S	In ₁₅ S ₂₉	3D	-

¹Double Diamond (see figure 2a). ²Diamond (see figure 3). ³ICF-24 topology (see figure 11a). ⁴ICF-25 topology (see figure 11b).



(a) ICF-24



(b) ICF-25

Figure 11: Representation of ICF-24 and ICF-25 topologies [38]

ICF-5 consists of T4 clusters as building units and presents two interpenetrating diamond-type lattices. ICF-17 presents the biggest cluster as building unit, the T5. Regarding the topology, ICF-17 presents the same as ICF-5. ICF-21 consists of the connection of T2 clusters into a non-interpenetrating diamond-type lattice and is the first selenium with a 4-connected, 3D structure. The ICF-22 structure is composed of two interpenetrating lattices, whose building block is a core-less T4 cluster. Both ICF-24 and ICF-25 present as building unit the T2 cluster and a spiro-5 unit. ICF-24 has a ring size of 20, being the first 4-connected, 3D framework with such ring size. ICF-25 also has a large pore size, having a ring size of 16. Like ICF-21, ICF-24 and ICF-25 have a 3D non-centrosymmetric framework structures. Regarding the last framework, ICF-27 presents a 6-connected network where the In₁₈S₄₁ clusters can be considered as the octahedral unit. Although there is enormous variability in terms of the clusters obtained, no structure was synthesised that had as a building unit the T3 cluster. According to Feng et al. [23], it is likely that for sulphur sites exposed to extra-framework inorganic cations the

coordination with other three M^{3+} becomes unfavourable due to the increase in bond valence sum, thus becoming unstable. As Loewenstein's rule, which states that the M^{4+}/M^{3+} ratio has to be higher than 1, is not fulfilled, the concentration of extra-framework mobile cations is higher, allowing the increase of ionic conductivity of the materials. As the synthesised structures present the limit situation, i.e. the M^{4+}/M^{3+} ratio is zero, as well as having an open porous system, the synthesised chalcogenides materials present a surprisingly high ionic conductivity.

Another example of a structure obtained without the use of organic compounds as structural agents is OCF-16 [71]. OCF-16 is based on the $P2Li_4In_{22}S_{44}$ cluster where Ca was used as counter-cation to stabilise the structure. As for the topology, it presents a double diamond topology. Due to the highly mobile extra-framework cations, ICF-16 presents a fast ion conductivity like the structures presented in [138].

Continuing the research in hydrated open framework chalcogenides, Zheng et al. [139] synthesised a sodium indium sulfide hydrate, called ICF-29 (see figure 12). The topology of this material can be derived from the perovskite, $CaTiO_3$. In order to obtain the ICF-29 structure from $CaTiO_3$ a triple substitution is performed: Ti^{4+} by SIn^{4+} , O^{2-} by InS_4^{5-} and Ca^{2+} by $Na_5(H_2O)_6^{5+}$. This material presents for the first time sulphur tetrahedrally bonded to four In ions. The remaining sulphurs have a 2-coordination, none with a 3-coordination. That absence is explained by the presence of the unusual SIn_4 unit. The existence of a tetracoordinated sulphur by four In ions can be explained by Brown's bond valence rule. The In-S bond length is slightly longer than expected ($2,55 \text{ \AA}$ instead of $2,44 \text{ \AA}$), so the valence sum is 2,24, close to the theoretical value of 2. This lengthening of the bond is explained by the fact that the remaining 3 In-S bonds involve bicoordinated sulphur, with a higher bond valence value than expected. The cavities of the synthesized material are occupied by $[Na_5(H_2O)_6]^{5+}$ clusters. Since the extra-framework species are highly ordered when compared to previously synthesised ICF materials, ICF-29 has a low ion conductivity.

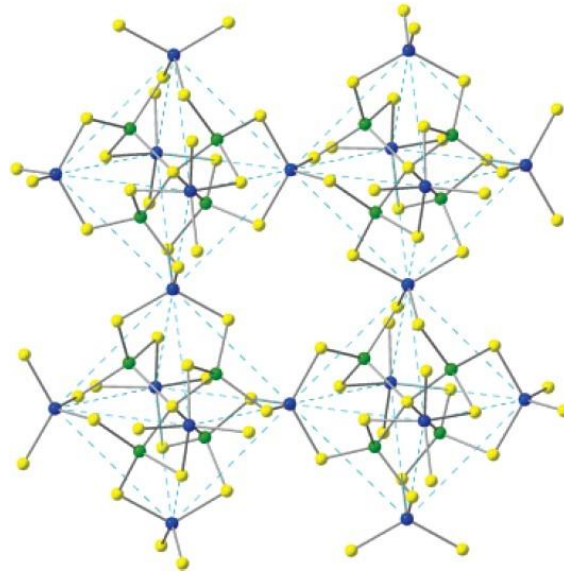


Figure 12: ICF-29 structure (blue: In^{3+} ; yellow: S^{2-} ; green: In^{3+} around tetrahedral S^{2-}) [139]

7 Hybrid Materials

Up to now most of the structures presented are composed by inorganic clusters that are connected by bicoordinated chalcogens atoms. However, it is possible to connect the different clusters through organic ligands, thus opening the doors to new materials with new physical and chemical properties. Due to the synergistic effect between the organic and inorganic components, such hybrid materials have unique optic and photochemical properties [25]. In 2010 Vaqueiro [140] published an extensive review on hybrid materials focused mainly on materials composed by clusters that had an organic component in their composition. Thus, although some examples of clusters with inorganic and organic components will be presented, the main focus will be on materials that present inorganic clusters connected through organic ligands, particularly recent publications, and materials that combine inorganic clusters with other materials such as graphene.

As for structures composed of clusters with inorganic and organic parts, several examples can be found in the literature. For structures composed by the simplest supertetrahedron, the T2, different topologies and chemical compositions were obtained. It is possible to find examples of 1D [141] [142], 2D [143] or 3D [144] [145] structures composed of T2 clusters that combine organic and inorganic components. For larger clusters, it is possible to find several examples of hybrid materials consisting of P1 [146] [147], C1 [146] [148], C2 [149] and a combination of P1 and C1 clusters [146]. Some of the structures obtained have interesting characteristics, namely the presence of chiral quartz-type topology [146] [147], interesting photoelectric properties [148] or the use of metal-chelate dyes as template, thus obtaining materials with optically active guest species [149].

The use of organic species is one of the strategies used to obtain isolated clusters, since the presence of the organic components allows the stabilisation of the negative charges of clusters, especially in large clusters. Wu et al. [150] obtained a family of isolated clusters, from T3 to T5, where the four corners of the clusters were connected to 1,5-diazabicyclo[4.3.0]non-5-ene or 1-methylimidazole. Another example of isolated clusters that are stabilised due to the presence of organic molecules in the vertices is the T3 Gallium Sulfide obtained by Vaqueiro et al. [151].

For materials composed of clusters that are connected by organic compounds, these may present a uni, bi- or three-dimensional architecture.

Xie et al. [152] obtained a 1D zig-zag structure composed of P1 clusters that are connected by dipyridyl ligands. Other examples of one-dimensional hybrid materials composed by clusters of the C_n or P_n series were obtained by Zheng et al. [153] and Zhang et al. [154]. Evaluating the optical properties of the different materials obtained, Zheng et al. [153] observed that such materials present optical size-dependent properties. Larger clusters lead to a red shift into longer wavelengths in the optical absorption spectra and superlattices show a broader absorption spectra in comparison to discrete clusters. The materials obtained by Zhang et al. [154] used tetrahedral quadridentate linkers to connect the different clusters, for the first time.

For two-dimensional structures, Zheng et al. [155] obtained layered materials consisting of

cadmium C_n type clusters and Xu et al. [156], also using cadmium, obtained a hybrid layered tellurium-based structure where T3 clusters were connected through 4,4'-trimethylenedipyridine. Continuing research on cadmium hybrid materials, Chen et al. [157] obtained a two-dimensional structure where the cadmium sulfide C1 clusters are connected by tetrakis(imidazolyl)borate ligands.

Vaqueiro et al. [158] obtained a two-dimensional structure with a honeycomb topology composed by T3 Ga-S clusters which were connected through 1,2-di(4-pyridyl)ethylene. Subsequently, the same team of researchers obtained chiral nanotubes and a two-dimensional structure where each T3 cluster is connected to other 4 T3 clusters [159]. Some years later, a new type of hybrid super-supertetrahedral cluster was obtained [160]. This new type of cluster is obtained when each vertex of the tetrahedron is replaced by a hybrid T3 cluster and the centre of the tetrahedron is occupied by a T3 cluster. The 5 T3 clusters are connect through bipyridyl ligands. Figure 13 shows a representation of the super-supertetrahedral obtained. Such clusters connect to each other through other bipyridyl ligands, forming a 2D framework with cross-shaped pores.

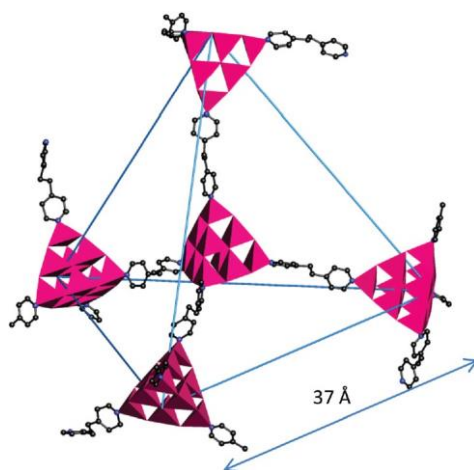


Figure 13: Super-supertetrahedral obtained by Vaqueiro et al. [160]

In the field of structures composed by oxyclusters, Yang et al. [94] obtained a laminar material, entitled IOS-1, composed by T5 In-O-S clusters that were connected by a carboxylate ligand thus presenting a honeycomb-like topology.

As for three-dimensional structures, the structures obtained by Lee et al. [79] and Jin et al. [81] mentioned above are the first examples of 3D structures composed by a combination of inorganic clusters and organic ligands. Manos et al. [161] obtained a structure composed of T2 clusters where each cluster was connected through a methylamine ligand. Another interesting characteristic of structure obtained is the presence of the $[Zn(H_2O)_4]^{2+}$ complexes as an extra framework species, acting as structure directing agent and counter cation. Wu et al. [162] were able to synthesise three-dimensional 4-connected structures where T3 or T4 clusters are connected by imidazolate. The different structures obtained present an interpenetrating diamond topology and the negative framework charge is counterbalanced by Li^+ cations and protonated 1,8-diazabicyclo[5.4.0]undec-7-ene molecules. Using imidazolate as an organic lig-

and, Zhang et al. [163] obtained a 3D structure, entitled SCIF-11, where the different T3 clusters were connected through the usual bicoordinated sulphur or through imidazolate, being one of the first materials where the existence of connection through inorganic and organic components was observed. An interrupted 3D structure, named SCIF-12, consisting of T4 clusters connected through imidazolate was also synthesised. Regarding the topology of synthesised materials, SCIF-11 presents a distorted double-interpenetrated diamond topology and SCIF-12 3,4-connected ins topology. For 3D structures composed by oxyclusters, a quartz chiral structure composed by T5 $\text{In}_{35}\text{S}_{48}\text{O}_8$ connected by imidazolate, named IOS-2, was synthesised by Yang et al. [94].

So far, materials consisting of clusters composed of organic and inorganic components or materials where inorganic clusters were connected by organic molecules have been presented. However, it is possible to find hybrid materials that consist of the coating of graphene, metals, TiO_2 or films with inorganic clusters. The presence of the heterojunction allows to improve the charge separation properties of the material, thus contributing to the increased efficiency of the hybrid material when it is used as a photocatalyst, for example.

Hou et al. [164] were able to deposit T4 isolated clusters (previous obtained in [55]) on reduced graphene oxide sheets. Regarding the optical properties of the composite, it can be observed that there is a small red-shift on the absorption edge and an enhanced absorption intensity when compared to the isolated clusters. Evaluating the photocurrent density, it is observed that, after the deposition of the graphene layer on the T4 clusters, a drastic increase occurs. The photocurrent density allows the evaluation of the separation efficiency of the photogenerated electron-hole pairs. Thus, the presence of the graphene phase improves the charge separation properties. Concerning the stability of the samples, it is observed that the isolated clusters decrease their photocurrent density over time. This phenomenon is called photocorrosion and is due to the self-oxidative deactivation of the cluster surface by the photogenerated holes. However, such a photocorrosion phenomenon is not observed in samples containing graphene. Therefore, the presence of graphene contributes to the improvement of the charge separation properties but also avoids photocorrosion of the final material.

Li et al. [165] deposited T5 Cu-In-S clusters on a TiO_2 electrode to produce photoelectrodes. Another example of a hybrid material that results from the combination of inorganic clusters with TiO_2 is the TiO_2 nanochips doped with T5 In-Cd-S clusters [166].

Liu et al. [167] explored the possibility of coating noble metal substrate with T n clusters in order to make the most of the semiconductor-metal heterojunction that forms. The noble metal chosen was silver in the shape of nanowires and it was chosen to use as a cluster the multimetallic T4 clusters with different metallic compositions previously obtained in [55]. Hu et al. [168] doped a BiVO_4 film with a T5 Cu-Ga-Sn clusters and evaluated the photochemical performance through the water splitting reaction.

It is also possible to find examples of materials that combine zeotype chalcogenide materials with metals or materials that presents organic molecules or nanoparticles confined into the

cavities.

Using the zeolitic-type materials previously obtained by Lin et al. [134], Mao et al. [169] were able to integrate TiO₂ nanowires with the CPM-121 structure. Comparing the current density of the hybrid material with the TiO₂ nanowires, it was observed that the photocurrent of the hybrid material is about three times higher and presents a higher activity both in the UV and in the visible light regions than of the isolated nanowires, thus showing the synergistic effect that exists between the semiconductor and metal materials.

Hu et al. [170] [171] were able to confine organic molecules into a zeotype chalcogenide material, for the purpose of designing a high efficient light-harvesting antennae. Due to the the semiconducting properties of the chalcogenide material, it is responsible to absorb the UV-light and pass the excited energy to the organic dyes molecules. Later, the same team of researchers [172] were able to confine Cu₂S nanoparticles into the cavities of the zeotype material previous obtained by Zheng et. al [16].

8 Alternative Methods of Synthesis

The materials presented so far were obtained through traditional methods of synthesis. The method that stands out is the hydro(solvo)thermal. This methodology, based on the use of polar solvents, organic amines and temperatures below 200°C, is currently the most used to prepare crystalline metal chalcogenides with various structures. However, more recently, two new methodologies, based on the use of ionic liquids and surfactants, have been developed to prepare such materials [3]. The need to look for new methodologies of synthesis arose from the growing interest in obtaining inorganic structures at room temperature or in solvent-free environments, hence taking into account the environmental and economic concerns that affect today's society [17].

8.1 Ionothermal Syntheses

An ionic liquid is a saltlike compound that melts below 100°C and that presents a pre-organized solvent structure. Since its discovery in 1914 [173], more than a thousand of ionic liquids have been produced and published and are now commercially available. Due to its unusual properties, quite different from the usual solvents, the interest in using ionic liquids for inorganic synthesis has grown lately [17] [174] [175] [176].

Cooper et al. [177] published the first example of the use of ionic liquids in the inorganic synthesis, acting as a solvent and as a template, of aluminophosphate zeotype frameworks. Compared to the use of conventional solvents, due to the low vapour pressure of ionic liquids, the synthesis does not need to be performed under high autogenous pressures, thus avoiding the safety concerns and the equipment costs associated with the use of autoclaves. When an ionic liquid is used as solvent and template, the competition that exists between the interaction of the solvent and template with the solid that is being formed is eliminated. Since the first use of ionic liquids to obtain inorganic structures, the ionothermal synthesis technique has been used to obtain zeolites, metal – organic frameworks and nanomaterials [175].

The synthesis of isolated T5 clusters was one of the first uses of ionothermal synthesis in the field of chalcogenide cluster-based materials [178]. Four distinct clusters were obtained with the Ga-Cu-S or In-Cu-S composition where 1-butyl-2,3-dimethylimidazolium chloride ([BmIm][Cl]) was used as an ionic liquid. The corners of the clusters have SH⁻, Cl⁻ or BIm⁺ groups that allow the stabilisation of the negative charge inherent to the cluster, preventing them from polymerization. Continuing research into obtaining large OD structures, Li et al. [179] obtained two new discrete molecular anions, ZBT-1 and ZBT-2, with a spherical shape. Such anions were obtained using Ge₄Se₁₀ as a precursor, SnCl₄ · 5 H₂O as a Sn source and 1-butyl-3-methylimidazolium tetrafluoroborate ([BmIm][BF₄]) or 1-butyl-2,3-dimethylimidazolium tetrafluoroborate [BmmIm][BF₄] as an ionic liquid. The structures are based on two clusters as building units: Ge₃Se₉, a fragment of the tetrahedral precursor Ge₄Se₁₀, and Sn₆Se₁₈, two semi-cubes clusters that are connected by two Se. Regarding the architecture of the structures, it can be simplified in a truncated dodecahedron with a large spherical cavity, with dimensions similar to the FAU supercage (see figure 14).

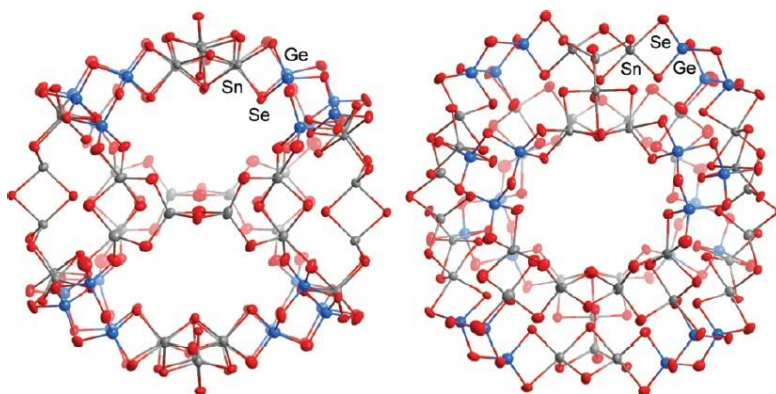


Figure 14: Different orientations of ZBT-1 [179]

Due to the growing interest in obtaining isolated clusters for photocatalysis applications, T3 In-Q (Q = S, Se, S/Se) clusters [180], T4 In-Cd-Q (Q = S, Se, S/Se, Te/Se) clusters [181] and T5 In-Cu-Q (Q = Se, S/Se) clusters [182] were recently obtained.

Regarding 2D structures, Santner et al. [183] obtained it using P1 cluster Mn₄Sn₄Se₁₇ as a precursor and treating it with 1,2-diaminoethane in [BmIm][BF₄]. The structure obtained can be seen as a honeycomb network with heavily distorted hexagonal rings composed by Sn₃Se₄ clusters.

Moving on to structures with higher dimensions, Li et al. [184] obtained the first three-dimensional structures using ionothermal synthesis as a synthesis procedure. By adding small amounts of hydrazine to the reaction medium containing imidazolium chlorides as the ionic liquid, different 3D structures based on Sn-Se were obtained. By changing the relative amount of hydrazine, as well as the length of the carbon chain of the ionic liquid ([BmIm]⁺, 1-butyl-3-methyl imidazolium, [BmmIm]⁺, 1-butyl-2,3-dimethyl imidazolium, or [PmmIm]⁺, 1-pentyl-2,3-dimethyl imidazolium) it was possible to obtain three distinct structures, all of them having

Sn_3Se_4 semicubes as building units. The structure of the first compound (see figure 15a) can be simplified into infinite Sn-Se chains that are connected to each other, resulting in a 3D structure with multi directional channels filled with $[\text{BmIm}]^+$ cations. As for the second structure (see figure 15b), it also presents multi directional channels filled with $[\text{BmmIm}]^+$ cations. However, it presents a different connection mode between the Sn_3Se_4 semicubes clusters. Each Sn_3Se_4 semicube is connected alternately with SnSe_4 or $\text{SnSe}_3(\text{Se}_2)_0 \cdot 9\text{Se}_0 \cdot 1$. Has for the third structure, it has a similar structure than the second compound. In this case, the channels are filled with $[\text{PmmIm}]^+$ cations instead of $[\text{BmmIm}]^+$. When the relative amount of hydrazine increases in the gel that gives rise to the third compound, a layered compound rather than a 3D structure is formed.

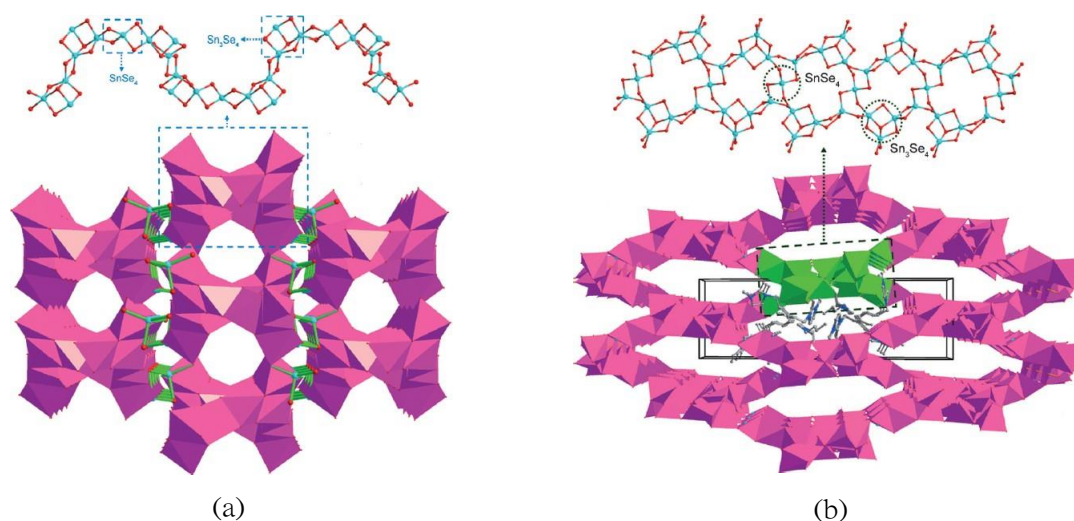


Figure 15: Representation of of the 3D structures obtained in [184]

Lin et al. [185] were able to synthesise a 3D material, also composed by Sn and Se, where $[\text{BmIm}][\text{BF}_4]$ was used as an ionic liquid, not being necessary the use of hydrazine in the reaction medium. The building unit of this structure is once again the Sn_3Se_4 semicube, presenting three distinct means of connection between the clusters, originating a 3D structure with a complex system of channels responsible for the extra-large microporosity of the sample. When there is the replacement of $[\text{BmIm}][\text{BF}_4]$ with 1-Ethyl-3-methyl-imidazolium-bromide ($[\text{EmIm}][\text{Br}]$) a layered material with the framework previous describe in [91] is obtained.

It is possible, through ionothermal synthesis, to obtain new structures using existing 3D structures as a precursor. Lin et al. [186] observed that when a heat treatment is applied to the 3D $\text{K}_2\text{Sn}_2\text{Se}_5$ structure it undergoes a deconstruction, reducing to a 1D structure, passing through a 2D structure. When a heat treatment is applied again to the 1D structure, but this time in the presence of amines, a 3D structure different from $\text{K}_2\text{Sn}_2\text{Se}_5$ is obtained. It is concluded that although temperature is the determining factor in the transformation of the structures, the amines influence the breakage and reconstruction of the Sn-Se bonds.

After the first synthesis of these structures, Lin et al. [187] conducted a more in-depth study of the Sn/Ge/Se system in the presence of ionic liquids. With different experimental

conditions, i.e. different amount of amines, it was possible to obtain structures from 0D to 3D. It was observed that the amount of amines in the reaction medium has a direct influence on the chemical composition and on the dimension of the final structure, thus allowing the customisation of the optical properties of the final material. The importance of amines in the reaction was also observed by other authors who were able to obtain heterometallic structures through the insertion of Ag [188] or Mn [189] into the Sn-Se system. Li et al. [188] obtained six different structures by varying the amount of amines, temperature and time of synthesis. Of the structures obtained, the laminar structure composed by Ag, Sn and Se stands out, since heterometallic structures with Ag are not common. The structure of this compound can be simplified into Sn and Se double chains connected by Ag, thus forming a laminar structure (see figure 16).

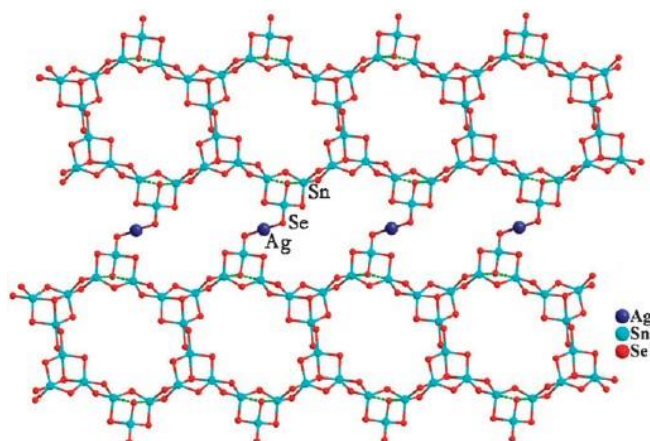


Figure 16: Representation of the Sn-Ag-Se laminar material obtained in [188]

Regarding the structures based on the combination of Sn-Mn-Se, Du et al. [189] were able to obtain such structures by adding $\text{MnCl}_2 \cdot 4 \text{H}_2\text{O}$ to the reaction medium. Changing the amount of ionic liquid used, as well as the type of amine used, four structures were obtained. All structures obtained are layered, with the Sn_3Se_4 semicube as building units, differing in the ring size and the type of compound that exists in the inter layered space. When only metal-amine complexes are found in the space between layers, laminar structures with elliptical six-membered rings are obtained (structures 1 and 2 at the figure 17). When the space between layers is occupied by a mixture of metal-amine complexes and ionic liquid cations, the materials obtained have distorted hexagonal rings. When ethylenediamine (en) is used as the amine a structure with an eight-membered heart-shaped ring is obtained (structure 3 at the figure 17). When the amine is replaced by diethylenetriamine (dien) the structure obtained consists of both eight-membered heart-shaped rings and compressed six-membered rings (structure 4 at the figure 17). It is thus observed that when the metal-amine complex is the only structuring agent the amine used does not influence the final structure. When there is a competition between the metal-complex and the ionic liquid as structuring agents, the final structure obtained is influenced by the amine used.

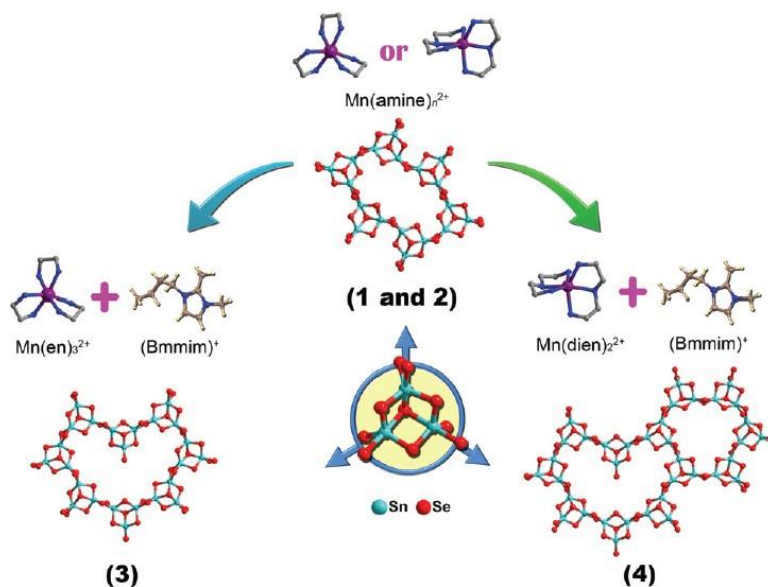


Figure 17: Different 2D materials obtained by [189], with focus on the components that are in the interlayer space

Continuing the research on this subject, Santner et al. [190] evaluated the influence that the ionic liquid anion has on the final structure as well as the temperature of synthesis. To this end, structures were synthesised in which ion liquids with different BX_4 anions were used: BF_4 and B(CN)_4 . When $[\text{BmmIm}][\text{BF}_4]$ is used as an ionic liquid, it is fully incorporated in the final 3D structure. However, when $[\text{EmIm}][\text{B(CN)}_4]$ is used as ionic liquid at low temperatures, there is no presence of the ionic liquid in the structure, obtaining a 2D structure with a low distance between layers.

8.2 Surfactant-thermal Method

Surfactants are organic compounds containing hydrophilic groups, which tend to be soluble in water, and hydrophobic groups, usually composed of hydrocarbon chains and are typically insoluble in water. This type of compounds has been widely used in the preparation of nanocrystals and mesoporous materials. In the case of nanocrystals it is possible to tailor the size, shape and surface properties of the nanoparticles. In the case of mesoporous frameworks, it allows to control the pore size and phase of porous materials [3] [191] [192].

Since surfactants can control the morphology of materials at micro scale, studies are currently being carried out to investigate the possibility of using surfactants as structuring direct agents or solvents. Compared to traditional solvents, surfactants have low vapour pressure and high thermal stability. With respect to ionic liquids, another class of materials that has been the target of studies for presenting excellent properties as a solvent in the synthesis of inorganic crystalline materials, surfactants present numerous advantages, namely low cost, great commercial availability and different properties (cationic, anionic, neutral, basic or acidic) [191] [192].

One of the first examples of chalcogenide materials prepared using surfactant is a lamellar tin sulfide compound [193] [194]. Later, some crystalline lamellar materials based on Sn_2S_6 dimer [195], $\text{Ge}_4\text{S}_{10}^{4-}$ T2 cluster [196] [197] [198], $\text{Ge}_4\text{Se}_{10}^{4-}$ T2 cluster [199] or $\text{Cd}_8\text{Se}(\text{SePh})_{12}\text{Cl}_4^{2-}$ P1 cluster [200] were also obtained.

Wacchold et al. [199], when obtained the laminar materials based on $\text{Ge}_4\text{Se}_{10}^{4-}$, also evaluated how the surfactant alkyl chain length and the presence of N-H groups on the surfactant influence the final structure. Regarding the alkyl chain length, it was observed that there is a change on the spatial arrangement of the material when using a surfactant with a alkyl chain composed by more than 9 carbons. When a surfactant with a N-H is used, isolated adamantane clusters are obtained instead of a lamellar material.

All the materials presented so far use surfactants as reagent. Xiong et al. [201] used for the first time surfactants as a reaction medium to obtain chalcogenic materials. Using chalcogenidoarsenates as a model system, 0D, 1D, 2D and 3D structures were obtained. When no surfactant was used on the reaction media, no type of structure was obtained, thus showing the fundamental role of surfactants in obtaining such structures. Now using mercury selenidostannates instead of chalcogenidoarsenates as a model system, the same team of researchers observed that the use of PEG-400 in such a chemical system allows to kinetically transform between two thermodynamically stable 1D phases [202]. Continuing the research in this area, a 2D antimony oxosulfide was synthesised and its H_2 photoproduction through water splitting was verified [203]. Zhang et al. [204] made several syntheses where they evaluated the consequences in the final material of placing surfactants and amines, compounds used as structural directing agents, in the reaction medium. Different amines were used and, depending on the amine, different structures were obtained. Using PEG-400 as a reaction medium, a 2D material based on the $\text{MnGe}_2\text{S}_8\text{N}_2$ trimer was obtained when using hydrazine as amine. By replacing hydrazine with ethylenediamine a quasi-layered material consisting of T2 $\text{MnGe}_3\text{Se}_{10}$ clusters is obtained. When 1,2-propanediamine or 1,3-propanediamine is used, a 1D chain composed of Ge_2Se_7 or MnGeSe_6 dimers is obtained, respectively. When the surfactant is replaced by another solvent no structure is obtained. Shen et al. [205], using the A-Cu-Sb-S (A = Rb, Cs) chemical system and PEG-400 as a reaction media, obtained for the first time two new 3D structures. The use of surfactants also makes it possible to obtain nanocomposites with unique characteristics. Xiong et al. [206] obtained a nanocomposite that consists of Sn_3Se_7 layers with PEG chains into its nanochannels (see figure 18). Usually in this type of materials the polymers are located between the layers of the inorganic material, and not in the channels of the structure (see figure 18b).

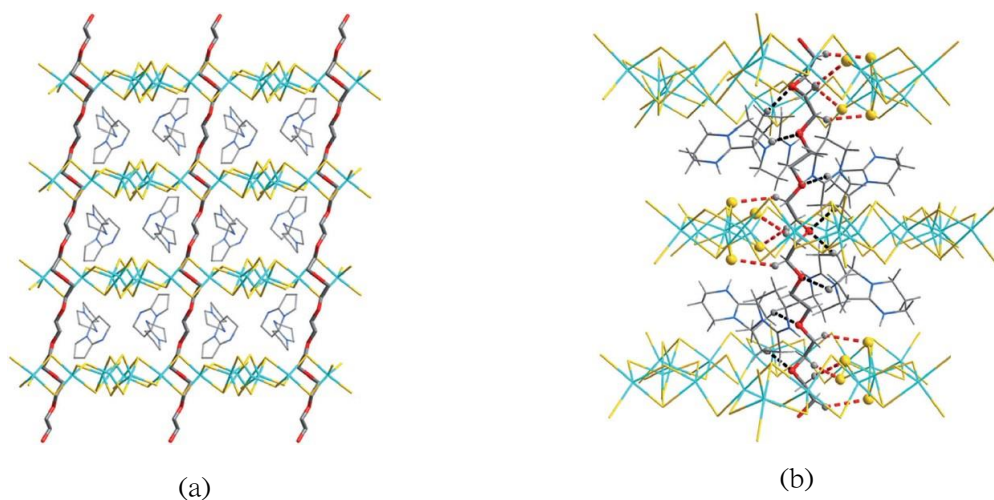


Figure 18: Representation of of the 2D structures obtained in [206] (blue - Sn; yellow - Se; black - C; red - O)

References

- [1] A. Fujishima and K. Honda, "Electrochemical photolysis of water at a semiconductor electrode," *Nature*, vol. 238, pp. 37 – 38, 1972.
- [2] S. Chandrasekaran, L. Yao, L. Deng, C. Bowen, Y. Zhang, S. Chen, Z. Lin, F. Peng, and P. Zhang, "Recent advances in metal sulfides: from controlled fabrication to electrocatalytic, photocatalytic and photoelectrochemical water splitting and beyond," *Chem. Soc. Rev.*, vol. 48, pp. 4178 – 4280, 2019.
- [3] L. Nie and Q. Zhang, "Recent progress in crystalline metal chalcogenides as efficient photocatalysts for organic pollutant degradation," *Inorganic Chemistry Frontiers*, vol. 4, no. 12, pp. 1953 – 1962, 2017.
- [4] M. A. A. S. Yong Xu, "The absolute energy positions of conduction and valence bands of selected semiconducting minerals," *American Mineralogist*, vol. 85, pp. 543 – 556, 2000.
- [5] K. Kobayakawa, A. Teranishi, T. Tsurumaki, Y. Sato, and A. Fujishima, "Photocatalytic activity of CuIn_2S_4 and CuIn_5S_8 ," *Electrochimica Acta*, vol. 37, pp. 465 – 467, 1992.
- [6] Z. Lei, W. You, M. Liu, G. Zhou, T. Takata, M. Hara, K. Domen, and C. Li, "Photocatalytic water reduction under visible light on a novel ZnIn_2S_4 catalyst synthesized by hydrothermal method," *Chemical communications (Cambridge, England)*, no. 17, pp. 2142 – 2143, 2003.
- [7] Di Chen and J. Ye, "Photocatalytic H_2 evolution under visible light irradiation on AgIn_5S_8 photocatalyst," *Journal of Physics and Chemistry of Solids*, vol. 68, no. 12, pp. 2317 – 2320, 2007.

- [8] Z. Chen, D. Li, W. Zhang, C. Chen, W. Li, M. Sun, Y. He, and X. Fu, “Low-temperature and template-free synthesis of Zn₂S₄ microspheres,” *Inorganic Chemistry*, vol. 47, no. 21, pp. 9766 – 9772, 2008.
- [9] W. Li, D. Li, Z. Chen, H. Huang, M. Sun, Y. He, and X. Fu, “High-efficient degradation of dyes by Zn_{1-x}Cd_xS solid solutions under visible light irradiation,” *The Journal of Physical Chemistry C*, vol. 112, no. 38, pp. 14943 – 14947, 2008.
- [10] Y. Li, X. He, and M. Cao, “Micro-emulsion-assisted synthesis of ZnS nanospheres and their photocatalytic activity,” *Materials Research Bulletin*, vol. 43, no. 11, pp. 3100 – 3110, 2008.
- [11] M. Sun, D. Li, W. Li, Y. Chen, Z. Chen, Y. He, and X. Fu, “New photocatalyst, Sb₂S₃, for degradation of methyl orange under visible-light irradiation,” *The Journal of Physical Chemistry C*, vol. 112, no. 46, pp. 18076 – 18081, 2008.
- [12] Y. He, D. Li, G. Xiao, W. Chen, Y. Chen, M. Sun, H. Huang, and X. Fu, “A new application of nanocrystal in Sb₂S₃ in efficient degradation of organic pollutants under visible light irradiation,” *The Journal of Physical Chemistry C*, vol. 113, no. 13, pp. 5254 – 5262, 2009.
- [13] W. Zhang, D. Li, M. Sun, Y. Shao, Z. Chen, G. Xiao, and X. Fu, “Microwave hydrothermal synthesis and photocatalytic activity of Ag₂S for the degradation of dye,” *Journal of Solid State Chemistry*, vol. 183, no. 10, pp. 2466 – 2474, 2010.
- [14] M. E. Davis, “Ordered porous materials for emerging applications,” *Nature*, vol. 417, p. 813 – 821, 2002.
- [15] N. Zheng, X. Bu, B. Wang, and P. Feng, “Open-framework chalcogenides as visible-light photocatalysts for hydrogen generation from water,” *Angewandte Chemie*, vol. 44, pp. 5299 – 5303, 2005.
- [16] N. Zheng, X. Bu, B. Wang, and P. Feng, “Microporous and photoluminescent chalcogenide zeolite analogs,” *Science*, vol. 298, no. 5602, pp. 2366 – 2369, 2002.
- [17] S. Santner, J. Heine, and S. Dehnen, “Synthesis of crystalline chalcogenides in ionic liquids,” *Angewandte Chemie (International ed. in English)*, vol. 55, no. 3, pp. 876 – 893, 2016.
- [18] C.-H. Lai, M.-Y. Lu, and L.-J. Chen, “Metal sulfide nanostructures: synthesis, properties and applications in energy conversion and storage,” *J. Mater. Chem.*, vol. 22, pp. 19 – 30, 2012.
- [19] Y. Zhao and C. Burda, “Development of plasmonic semiconductor nanomaterials with copper chalcogenides for a future with sustainable energy materials,” *Energy Environ. Sci.*, vol. 5, pp. 5564 – 5576, 2012.

- [20] X.-Y. Yu, Le Yu, and X. W. D. Lou, "Metal sulfide hollow nanostructures for electrochemical energy storage," *Advanced Energy Materials*, vol. 6, no. 3, p. 1501333, 2016.
- [21] C. Coughlan, M. Ibáñez, O. Dobrozhan, A. Singh, A. Cabot, and K. M. Ryan, "Compound copper chalcogenide nanocrystals," *Chemical Reviews*, vol. 117, no. 9, pp. 5865 – 6109, 2017. PMID: 28394585.
- [22] P. Geng, S. Zheng, H. Tang, R. Zhu, L. Zhang, S. Cao, H. Xue, and H. Pang, "Transition metal sulfides based on graphene for electrochemical energy storage," *Advanced Energy Materials*, vol. 8, no. 15, p. 1703259, 2018.
- [23] P. Feng, X. Bu, and N. Zheng, "The interface chemistry between chalcogenide clusters and open framework chalcogenides," *Accounts of Chemical Research*, vol. 38, no. 4, pp. 293 – 303, 2005. PMID: 15835876.
- [24] C. L. Cahill and J. B. Parise, "On the formation of framework indium sulfides," *J. Chem. Soc., Dalton Trans.*, pp. 1475 – 1482, 2000.
- [25] I. Dance and K. Fisher, *Metal Chalcogenide Cluster Chemistry*, vol. 41, p. 637 – 803. John Wiley, 1994.
- [26] R. L. Bedard, L. D. Vail, S. T. Wilson, and E. M. Flanigen, "Crystalline microporous metal sulfide compositions," December 6, 1988, US 4,880,761.
- [27] R. Bedard, S. Wilson, L. Vail, J. Bennett, and E. Flanigen, "The next generation: Synthesis, characterization, and structure of metal sulfide-based microporous solids," in *Zeolites: Facts, Figures, Future Part A - Proceedings of the 8th International Zeolite Conference* (P. Jacobs and R. van Santen, eds.), vol. 49 of *Studies in Surface Science and Catalysis*, pp. 375 – 387, Elsevier, 1989.
- [28] R. W. Scott, M. J. MacLachlan, and G. A. Ozin, "Synthesis of metal sulfide materials with controlled architecture," *Current Opinion in Solid State and Materials Science*, vol. 4, no. 2, pp. 113 – 121, 1999.
- [29] H. Li, A. Laine, M. O' Keeffe, and O. M. Yaghi, "Supertetrahedral sulfide crystals with giant cavities and channels," *Science*, vol. 283, no. 5405, pp. 1145 – 1147, 1999.
- [30] H. Li, J. Kim, T. L. Groy, M. O' Keeffe, and O. M. Yaghi, "20 Å cd₄in₁₆s₃₅14- supertetrahedral t₄ clusters as building units in decorated cristobalite frameworks," *Journal of the American Chemical Society*, vol. 123, no. 20, pp. 4867 – 4868, 2001. PMID: 11457310.
- [31] G. Férey, "Supertetrahedra in sulfides: matter against mathematical series?," *Angewandte Chemie (International ed. in English)*, vol. 42, no. 23, pp. 2576 – 2579, 2003.
- [32] O. M. Yaghi, Z. Sun, D. A. Richardson, and T. L. Groy, "Directed transformation of molecules to solids: Synthesis of a microporous sulfide from molecular germanium sulfide cages," *Journal of the American Chemical Society*, vol. 116, no. 2, pp. 807 – 808, 1994.

- [33] K. Tan, A. Darovsky, and J. B. Parise, "Synthesis of a novel open-framework sulfide, $\text{Cu}_2\text{S}_5(\text{C}_2\text{H}_5)_4\text{n}$, and its structure solution using synchrotron imaging plate data," *Journal of the American Chemical Society*, vol. 117, no. 26, pp. 7039 – 7040, 1995.
- [34] K. Tan, Y. Ko, J. B. Parise, and A. Darovsky, "Hydrothermal growth of single crystals of tma-cugs-2 , $[\text{C}_4\text{H}_{12}\text{N}]_6[(\text{Cu}_{0.44}\text{Ge}_{0.56}\text{S}_{2.23})_4(\text{Ge}_4\text{S}_8)_3]$ and their characterization using synchrotron/imaging plate data," *Chemistry of Materials*, vol. 8, no. 2, pp. 448 – 453, 1996.
- [35] C. L. Bowes, W. U. Huynh, S. J. Kirkby, A. Malek, G. A. Ozin, S. Petrov, M. Twardowski, D. Young, R. L. Bedard, and R. Broach, "Dimetal linked open frameworks: $[(\text{CH}_3)_4\text{N}]_2(\text{Ag}_2\text{Cu}_2)\text{Ge}_4\text{S}_{10}$," *Chemistry of Materials*, vol. 8, no. 8, pp. 2147 – 2152, 1996.
- [36] C. L. Cahill, Y. Ko, J. C. Hanson, K. Tan, and J. B. Parise, "Structure of microporous quimngs-1 and in situ studies of its formation using time-resolved synchrotron x-ray powder diffraction," *Chemistry of Materials*, vol. 10, no. 5, pp. 1453 – 1458, 1998.
- [37] N. Zheng, X. Bu, and P. Feng, "Two-dimensional organization of $[\text{ZnGe}_3\text{S}_9(\text{H}_2\text{O})]_4$ supertetrahedral clusters templated by a metal complex," *Chem. Commun.*, pp. 2805 – 2807, 2005.
- [38] X. Bu, N. Zheng, and P. Feng, "Tetrahedral chalcogenide clusters and open frameworks," *Chemistry – A European Journal*, vol. 10, no. 14, pp. 3356 – 3362, 2004.
- [39] C. L. Cahill, Y. Ko, and J. B. Parise, "A novel 3-dimensional open framework sulfide based upon the $[\text{In}_{10}\text{S}_{20}]_{10}$ -supertetrahedron: dma-ins-sb1 ," *Chemistry of Materials*, vol. 10, no. 1, pp. 19 – 21, 1998.
- [40] H. Li, M. Eddaoudi, A. Laine, M. O'Keeffe, and O. M. Yaghi, "Noninterpenetrating indium sulfide supertetrahedral cristobalite framework," *Journal of the American Chemical Society*, vol. 121, no. 25, pp. 6096 – 6097, 1999.
- [41] N. Zheng, X. Bu, and P. Feng, "Nonaqueous synthesis and selective crystallization of gallium sulfide clusters into three-dimensional photoluminescent superlattices," *Journal of the American Chemical Society*, vol. 125, no. 5, pp. 1138 – 1139, 2003. PMID: 12553794.
- [42] W. Wang, H. Yang, M. Luo, Y. Zhong, D. Xu, T. Wu, and Z. Lin, "A 36-membered ring metal chalcogenide with a very low framework density," *Inorganic Chemistry*, vol. 56, no. 24, pp. 14730 – 14733, 2017. PMID: 29172507.
- [43] Z. Wu, M. Luo, C. Xue, J. Zhang, J. Lv, X. Wang, and T. Wu, "New 2d assemblage of supertetrahedral chalcogenide clusters with tetravalent-metal-induced interrupted sites," *Crystal Growth & Design*, vol. 19, no. 7, pp. 4151 – 4156, 2019.
- [44] W. Wang, X. Wang, D. Hu, H. Yang, C. Xue, Z. Lin, and T. Wu, "An unusual metal chalcogenide zeolitic framework built from the extended spiro-5 units with supertetrahe-

- dral clusters as nodes,” *Inorganic Chemistry*, vol. 57, no. 3, pp. 921 – 925, 2018. PMID: 29308887.
- [45] H. Ahari, A. Garcia, S. Kirkby, G. A. Ozin, D. Young, and A. J. Lough, “Self-assembling iron and manganese metal – germanium – selenide frameworks: $[nme_4]_2mge_4se_{10}$, where $m = fe$ or mn ,” *J. Chem. Soc., Dalton Trans.*, pp. 2023 – 2028, 1998.
- [46] C. Wang, X. Bu, N. Zheng, and P. Feng, “Indium selenide superlattices from $(in_{10}se_{18})_6$ supertetrahedral clusters,” *Chem. Commun.*, pp. 1344 – 1345, 2002.
- [47] C. Xue, J. Lin, H. Yang, W. Wang, X. Wang, D. Hu, and T. Wu, “Supertetrahedral cluster-based in – se open frameworks with unique polyselenide ion as linker,” *Crystal Growth & Design*, vol. 18, no. 5, pp. 2690 – 2693, 2018.
- [48] X. Bu, N. Zheng, X. Wang, B. Wang, and P. Feng, “Three-dimensional frameworks of gallium selenide supertetrahedral clusters,” *Angewandte Chemie (International ed. in English)*, vol. 43, no. 12, pp. 1502 – 1505, 2004.
- [49] P. Vaqueiro and M. L. Romero, “Three-dimensional gallium sulphide open frameworks,” *Journal of Physics and Chemistry of Solids*, vol. 68, no. 5, pp. 1239 – 1243, 2007. 7th International Conference of Solids State Chemistry 2006 (SSC 2006).
- [50] C. Wang, X. Bu, N. Zheng, and P. Feng, “A 3d open-framework indium telluride and its selenide and sulfide analogues,” *Angewandte Chemie (International ed. in English)*, vol. 41, pp. 1959 – 1961, 2002.
- [51] K. Tsamourtzi, J.-H. Song, T. Bakas, A. J. Freeman, P. N. Trikalitis, and M. G. Kanatzidis, “Straightforward route to the adamantane clusters $[sn_4q_{10}]_4$ ($q = s, se, te$) and use in the assembly of open-framework chalcogenides $(me_4n)_2m[sn_4se_{10}]$ ($m = mn_{ii}, fe_{ii}, co_{ii}, zn_{ii}$) including the first telluride member $(me_4n)_2mn[ge_4te_{10}]$,” *Inorganic Chemistry*, vol. 47, no. 24, pp. 11920 – 11929, 2008. PMID: 18998670.
- [52] Q. Zhang, I. Chung, J. I. Jang, J. B. Ketterson, and M. G. Kanatzidis, “A polar and chiral indium telluride featuring supertetrahedral t_2 clusters and nonlinear optical second harmonic generation,” *Chemistry of Materials*, vol. 21, no. 1, pp. 12 – 14, 2009.
- [53] X. Bu, N. Zheng, Y. Li, and P. Feng, “Templated assembly of sulfide nanoclusters into cubic- $c3n_4$ type framework,” *Journal of the American Chemical Society*, vol. 125, no. 20, pp. 6024 – 6025, 2003. PMID: 12785810.
- [54] C. Xue, L. Zhang, X. Wang, X. Wang, J. Zhang, and T. Wu, “Highly open chalcogenide frameworks built from unusual defective supertetrahedral clusters,” *Dalton Trans.*, vol. 48, pp. 10799 – 10803, 2019.
- [55] T. Wu, L. Wang, X. Bu, V. Chau, and P. Feng, “Largest molecular clusters in the supertetrahedral tn series,” *Journal of the American Chemical Society*, vol. 132, no. 31, pp. 10823 – 10831, 2010. PMID: 20681716.

- [56] C. Wang, Y. Li, X. Bu, N. Zheng, O. Zivkovic, C.-S. Yang, and P. Feng, "Three-dimensional superlattices built from (m₄in16s₃₃)₁₀- (m = mn, co, zn, cd) supertetrahedral clusters," *Journal of the American Chemical Society*, vol. 123, no. 46, pp. 11506 – 11507, 2001. PMID: 11707140.
- [57] Y.-H. Wang, M.-H. Zhang, Y.-M. Yan, G.-Q. Bian, Q.-Y. Zhu, and J. Dai, "Transition metal complexes as linkages for assembly of supertetrahedral t₄ clusters," *Inorganic Chemistry*, vol. 49, no. 21, pp. 9731 – 9733, 2010. PMID: 20919694.
- [58] T. Wu, X. Bu, X. Zhao, R. Khazhaky, and P. Feng, "Phase selection and site-selective distribution by tin and sulfur in supertetrahedral zinc gallium selenides," *Journal of the American Chemical Society*, vol. 133, no. 24, pp. 9616 – 9625, 2011. PMID: 21595469.
- [59] T. Wu, X. Wang, X. Bu, X. Zhao, Le Wang, and P. Feng, "Synthetic control of selenide supertetrahedral clusters and three-dimensional co-assembly by charge-complementary metal cations," *Angewandte Chemie (International ed. in English)*, vol. 48, no. 39, pp. 7204 – 7207, 2009.
- [60] D. Liu, X. Fan, X. Wang, D. Hu, C. Xue, Y. Liu, Y. Wang, X. Zhu, J. Guo, H. Lin, Y. Li, J. Zhong, D. Li, X. Bu, P. Feng, and T. Wu, "Cooperativity by multi-metals confined in supertetrahedral sulfide nanoclusters to enhance electrocatalytic hydrogen evolution," *Chemistry of Materials*, vol. 31, no. 2, pp. 553 – 559, 2019.
- [61] C. Wang, X. Bu, N. Zheng, and P. Feng, "Nanocluster with one missing core atom: a three-dimensional hybrid superlattice built from dual-sized supertetrahedral clusters," *Journal of the American Chemical Society*, vol. 124, no. 35, pp. 10268 – 10269, 2002. PMID: 12197715.
- [62] W. Su, X. Huang, J. Li, and H. Fu, "Crystal of semiconducting quantum dots built on covalently bonded t₅ [in₂₈cd₆s₅₄]-₁₂: the largest supertetrahedral cluster in solid state," *Journal of the American Chemical Society*, vol. 124, no. 44, pp. 12944 – 12945, 2002. PMID: 12405810.
- [63] X. Bu, N. Zheng, Y. Li, and P. Feng, "Pushing up the size limit of chalcogenide supertetrahedral clusters: two- and three-dimensional photoluminescent open frameworks from (cu₅in₃₀s₅₄)₁₃- clusters," *Journal of the American Chemical Society*, vol. 124, no. 43, pp. 12646 – 12647, 2002. PMID: 12392396.
- [64] T. Wu, Q. Zhang, Y. Hou, L. Wang, C. Mao, S.-T. Zheng, X. Bu, and P. Feng, "Monocopper doping in cd-in-s supertetrahedral nanocluster via two-step strategy and enhanced photoelectric response," *Journal of the American Chemical Society*, vol. 135, no. 28, pp. 10250 – 10253, 2013. PMID: 23819843.
- [65] J. Lin, Q. Zhang, L. Wang, X. Liu, W. Yan, T. Wu, X. Bu, and P. Feng, "Atomically precise doping of monomanganese ion into coreless supertetrahedral chalcogenide nanocluster

- inducing unusual red shift in Mn^{2+} emission,” *Journal of the American Chemical Society*, vol. 136, no. 12, pp. 4769 – 4779, 2014. PMID: 24625310.
- [66] X. Xu, W. Wang, D. Liu, D. Hu, T. Wu, X. Bu, and P. Feng, “Pushing up the size limit of metal chalcogenide supertetrahedral nanocluster,” *Journal of the American Chemical Society*, vol. 140, no. 3, pp. 888 – 891, 2018. PMID: 29337544.
- [67] L. Wang, T. Wu, F. Zuo, X. Zhao, X. Bu, J. Wu, and P. Feng, “Assembly of supertetrahedral t_5 copperindium sulfide clusters into a super-supertetrahedron of infinite order,” *Journal of the American Chemical Society*, vol. 132, no. 10, pp. 3283 – 3285, 2010. PMID: 20178361.
- [68] H. Li, J. Kim, M. O’ Keeffe, and O. M. Yaghi, “ $\text{Cd}_{16}\text{In}_6\text{S}_{13}$: A tetrahedron with a large cavity,” *Angewandte Chemie (International ed. in English)*, vol. 42, no. 16, pp. 1819 – 1821, 2003.
- [69] H. Wang, H. Yang, W. Wang, C. Xue, Y. Zhang, M. Luo, D. Hu, J. Lin, D. Li, and T. Wu, “Assembly of supertetrahedral clusters into a Cu-In-S superlattice via an unprecedented vertex – edge connection mode,” *CrystEngComm*, vol. 19, pp. 4709 – 4712, 2017.
- [70] L. Zhang, C. Xue, W. Wang, D. Hu, J. Lv, D. Li, and T. Wu, “Stable supersupertetrahedron with infinite order via the assembly of supertetrahedral t_4 zinc – indium sulfide clusters,” *Inorganic Chemistry*, vol. 57, no. 17, pp. 10485 – 10488, 2018. PMID: 30118223.
- [71] N. Zheng, X. Bu, and P. Feng, “Pentapusupertetrahedral clusters as building blocks for a three-dimensional sulfide superlattice,” *Angewandte Chemie (International ed. in English)*, vol. 43, no. 36, pp. 4753 – 4755, 2004.
- [72] C. Zimmermann, M. Melullis, and S. Dehnen, “Reactivity of chalcogenostannate salts: Unusual synthesis and structure of a compound containing ternary cluster anions $[\text{Co}_4(\text{M}_4\text{-se})(\text{SnSe}_4)_4]^{10-}$,” *Angewandte Chemie (International ed. in English)*, vol. 41, pp. 4269 – 4272, 2002.
- [73] S. Dehnen and M. K. Brandmayer, “Reactivity of chalcogenostannate compounds: syntheses, crystal structures, and electronic properties of novel compounds containing discrete ternary anions $[\text{Mii}_4(\mu_4\text{-se})(\text{SnSe}_4)_4]^{10-}$ ($\text{Mii} = \text{Zn, Mn}$),” *Journal of the American Chemical Society*, vol. 125, no. 22, pp. 6618 – 6619, 2003. PMID: 12769556.
- [74] N. Ding, D.-Y. Chung, and M. G. Kanatzidis, “ $\text{K}_6\text{Cd}_4\text{Sn}_3\text{Se}_{13}$: A polar open-framework compound based on the partially destroyed supertetrahedral $[\text{Cd}_4\text{Sn}_4\text{Se}_{17}]^{10-}$ cluster,” *Chem. Commun.*, pp. 1170 – 1171, 2004.
- [75] O. Palchik, R. G. Iyer, J. H. Liao, and M. G. Kanatzidis, “ $\text{K}_{10}\text{M}_4\text{Sn}_4\text{S}_{17}$ ($\text{M} = \text{Mn, Fe, Co, Zn}$): soluble quaternary sulfides with the discrete $[\text{M}_4\text{Sn}_4\text{S}_{17}]^{10-}$ supertetrahedral clusters,” *Inorganic Chemistry*, vol. 42, no. 17, pp. 5052 – 5054, 2003. PMID: 12924876.

- [76] M. J. Manos, R. G. Iyer, E. Quarez, J. H. Liao, and M. G. Kanatzidis, "SnZn₄Sn₄S₁₇₆: a robust open framework based on metal-linked penta-supertetrahedral zn₄sn₄s₁₇₁₀- clusters with ion-exchange properties," *Angewandte Chemie (International ed. in English)*, vol. 44, no. 23, pp. 3552 – 3555, 2005.
- [77] M. J. Manos, K. Chrissafis, and M. G. Kanatzidis, "Unique pore selectivity for cs⁺ and exceptionally high nh₄⁺ exchange capacity of the chalcogenide material k₆sn₄[zn₄sn₄s₁₇]," *Journal of the American Chemical Society*, vol. 128, no. 27, pp. 8875 – 8883, 2006. PMID: 16819882.
- [78] J. Lv, J. Zhang, C. Xue, D. Hu, X. Wang, D.-S. Li, and T. Wu, "Two penta- supertetrahedral cluster-based chalcogenide open frameworks: Effect of the cluster spa- tial connectivity on the electron-transport efficiency," *Inorganic Chemistry*, vol. 58, no. 6, pp. 3582 – 3585, 2019.
- [79] G. S. H. Lee, D. C. Craig, I. Ma, M. L. Scudder, T. D. Bailey, and I. G. Dance, "[s₄cd₁₇(sph)₂₈]₂-, the first member of a third series of tetrahedral [swmx(sr)y]z- clus- ters," *Journal of the American Chemical Society*, vol. 110, no. 14, pp. 4863 – 4864, 1988.
- [80] T. Vossmeier, G. Reck, L. Katsikas, E. T. K. Haupt, B. Schulz, and H. Weller, "A " double-diamond superlattice" built up of cd₁₇s₄(sch₂ch₂oh)₂₆ clusters," *Science*, vol. 267, no. 5203, pp. 1476 – 1479, 1995.
- [81] X. Jin, K. Tang, S. Jia, and Y. Tang, "Synthesis and crystal structure of a polymeric complex [s₄cd₁₇(sph)₂₄(ch₃ocs₂)_{4/2}]_n·nch₃oh," *Polyhedron*, vol. 15, no. 15, pp. 2617 – 2622, 1996.
- [82] N. Herron, J. C. Calabrese, W. E. Farneth, and Y. Wang, "Crystal structure and optical properties of cd₃₂s₁₄(sc₆h₅)₃₆. dmf₄, a cluster with a 15 angstrom cds core," *Science*, vol. 259, no. 5100, pp. 1426 – 1428, 1993.
- [83] T. Vossmeier, G. Reck, B. Schulz, L. Katsikas, and H. Weller, "Double-layer superlat- tice structure built up of cd₃₂s₁₄(sch₂ch₂(oh)ch₃)₃₆.cntdot.4h₂o clusters," *Journal of the American Chemical Society*, vol. 117, no. 51, pp. 12881 – 12882, 1995.
- [84] S. Behrens, M. Bettenhausen, A. C. Deveson, A. Eichhöfer, D. Fenske, A. Lohde, and U. Woggon, "Synthesis and Structure of the Nanoclusters [Hg₃₂Se₁₄(SePh)₃₆], [Cd₃₂Se₁₄(SePh)₃₆-(PPh₃)₄], [P(Et)₂(Ph)₄C₄H₈OSiMe₃]₅- [Cd₁₈I₁₇(PSiMe₃)₁₂], and [N(Et)₃C₄H₈OSiMe₃]₅[Cd₁₈I₁₇(PSiMe₃)₁₂]," *Angewandte Chemie International Edition in English*, vol. 35, no. 19, pp. 2215 – 2218, 1996.
- [85] A. Eichhöfer, P. T. Wood, R. N. Viswanath, and R. A. Mole, "Synthesis, struc- ture and physical properties of the manganese(ii) selenide/selenolate cluster complexes [mn₃₂se₁₄(seph)₃₆(pnpr₃)₄] and [na(benzene-15-crown-5)(c₄h₈o)₂]₂[mn₈se(seph)₁₆]," *Chem. Commun.*, pp. 1596 – 1598, 2008.

- [86] N. Zheng, X. Bu, H. Lu, Q. Zhang, and P. Feng, “Crystalline superlattices from single- sized quantum dots,” *Journal of the American Chemical Society*, vol. 127, no. 34, pp. 11963 – 11965, 2005. PMID: 16117534.
- [87] Q. Lin, X. Bu, and P. Feng, “An infinite square lattice of super-supertetrahedral t6-like tin oxyselenide clusters,” *Chem. Commun.*, vol. 50, pp. 4044 – 4046, 2014.
- [88] W. Schiwy and B. Krebs, “Sn₁₀O₄S₂₀ 8-: A new type of polyanion,” *Angewandte Chemie (International ed. in English)*, vol. 14, p. 436, 1975.
- [89] T. Kaib, M. Kapitein, and S. Dehnen, “Synthesis and crystal structure of [Li₈(H₂O)₂₉]-[Sn₁₀O₄S₂₀]-2H₂O,” *Zeitschrift für anorganische und allgemeine Chemie*, vol. 637, no. 12, pp. 1683 – 1686, 2011.
- [90] J. B. Parise and Y. Ko, “Material consisting of two interwoven 4-connected networks: Hydrothermal synthesis and structure of [Sn₅S₉O₂][Hn(CH₃)₃]₂,” *Chemistry of Materials*, vol. 6, no. 6, pp. 718 – 720, 1994.
- [91] J. B. Parise, Y. Ko, K. Tan, D. M. Nellis, and S. Koch, “Structural evolution from tin sulfide (selenide) layered structures to nove 3- and 4- connected tin oxy sulfides,” *Journal of Solid State Chemistry*, vol. 117, pp. 219 – 228, 1995.
- [92] S.-L. Huang, L. He, E.-X. Chen, H.-D. Lai, J. Zhang, and Q. Lin, “A wide pH-range stable crystalline framework based on the largest tin-oxysulfide cluster [Sn₂₀O₁₀S₃₄],” *Chem. Commun.*, vol. 55, pp. 11083 – 11086, 2019.
- [93] X.-M. Zhang, D. Sarma, Y.-Q. Wu, L. Wang, Z.-X. Ning, F.-Q. Zhang, and M. G. Kanatzidis, “Open-framework oxysulfide based on the supertetrahedral [In₄Sn₁₆O₁₀S₃₄]₁₂ – cluster and efficient sequestration of heavy metals,” *Journal of the American Chemical Society*, vol. 138, no. 17, pp. 5543 – 5546, 2016. PMID: 27082786.
- [94] H. Yang, J. Zhang, M. Luo, W. Wang, H. Lin, Y. Li, D. Li, P. Feng, and T. Wu, “The largest supertetrahedral oxychalcogenide nanocluster and its unique assembly,” *Journal of the American Chemical Society*, vol. 140, no. 36, pp. 11189 – 11192, 2018. PMID: 30088766.
- [95] Y. Zhang, X. Wang, D. Hu, C. Xue, W. Wang, H. Yang, D. Li, and T. Wu, “Monodisperse ultrasmall manganese-doped multimetallic oxysulfide nanoparticles as highly efficient oxygen reduction electrocatalyst,” *ACS Applied Materials & Interfaces*, vol. 10, no. 16, pp. 13413 – 13424, 2018. PMID: 29613757.
- [96] H. Ahari, A. Lough, S. Petrov, G. A. Ozin, and R. L. Bedard, “Modular assembly and phase study of two- and three-dimensional porous tin(IV) selenides,” *J. Mater. Chem.*, vol. 9, pp. 1263 – 1274, 1999.
- [97] T. Wu, F. Zuo, L. Wang, X. Bu, S.-T. Zheng, R. Ma, and P. Feng, “A large indium sulfide supertetrahedral cluster built from integration of ZnS-like tetrahedral shell with

- nacl-like octahedral core,” *Journal of the American Chemical Society*, vol. 133, no. 40, pp. 15886 – 15889, 2011. PMID: 21923195.
- [98] W. Wang, X. Wang, J. Zhang, H. Yang, M. Luo, C. Xue, Z. Lin, and T. Wu, “Three-dimensional superlattices based on unusual chalcogenide supertetrahedral in – sn – s nanoclusters,” *Inorganic Chemistry*, vol. 58, no. 1, pp. 31 – 34, 2019.
- [99] X. Han, Z. Wang, D. Liu, J. Xu, Y. Liu, and C. Wang, “Co-assembly of a three-dimensional open framework sulfide with a novel linkage between an oxygen-encapsulated t3 cluster and a supertetrahedral t2 cluster,” *Chem. Commun.*, vol. 50, pp. 796 – 798, 2014.
- [100] L. Wang, T. Wu, X. Bu, X. Zhao, F. Zuo, and P. Feng, “Coassembly between the largest and smallest metal chalcogenide supertetrahedral clusters,” *Inorganic Chemistry*, vol. 52, no. 5, pp. 2259 – 2261, 2013. PMID: 23421915.
- [101] J. Zhang, X. Liu, Y. Ding, C. Xue, and T. Wu, “Three new metal chalcogenide open frameworks built through co-assembly and/or hybrid assembly from supertetrahedral t5- inos and t3-ins nanoclusters,” *Dalton Trans.*, vol. 48, pp. 7537 – 7540, 2019.
- [102] H. Wang, W. Wang, D. Hu, M. Luo, C. Xue, D. Li, and T. Wu, “Hybrid assembly of different-sized supertetrahedral clusters into a unique non-interpenetrated mn – in – s open framework with large cavity,” *Inorganic Chemistry*, vol. 57, no. 11, pp. 6710 – 6715, 2018. PMID: 29792414.
- [103] Q. Zhang, X. Bu, L. Han, and P. Feng, “Two-dimensional indium sulfide framework constructed from pentasupertetrahedral p1 and supertetrahedral t2 clusters,” *Inorganic Chemistry*, vol. 45, no. 17, pp. 6684 – 6687, 2006. PMID: 16903723.
- [104] W. Wang, H. Yang, C. Xue, M. Luo, J. Lin, D. Hu, X. Wang, Z. Lin, and T. Wu, “The first observation on dual self-closed and extended assembly modes in supertetrahedral t3 cluster based open-framework chalcogenide,” *Crystal Growth & Design*, vol. 17, no. 6, pp. 2936 – 2940, 2017.
- [105] J. B. Parise, “Novel sulphide frameworks: synthesis and x-ray structural characterization of cs6sb10s18·1.2h2o,” *J. Chem. Soc., Chem. Commun.*, pp. 1553 – 1554, 1990.
- [106] J. B. Parise, “An antimony sulfide with a two-dimensional, intersecting system of channels,” *Science*, vol. 251, no. 4991, pp. 293 – 294, 1991.
- [107] J. B. Parise and Y. Ko, “Novel antimony sulfides: synthesis and x-ray structural characterization of sb3s5.n(c3h7)4 and sb4s7.n2c4h8,” *Chemistry of Materials*, vol. 4, no. 6, pp. 1446 – 1450, 1992.
- [108] T. Jiang, G. A. Ozin, and R. L. Bedard, “Nanoporous tin(IV) sulfides: Mode of formation,” *Advanced Materials*, vol. 6, pp. 860 – 865, 11 1994.

- [109] T. Jiang, G. A. Ozin, and R. L. Bedard, "Nanoporous tin(IV) sulfides: Thermochemical properties," *Advanced Materials*, vol. 7, pp. 166 – 170, 1995.
- [110] T. Jiang, A. J. Lough, G. A. Ozin, D. Young, and R. L. Bedard, "Synthesis and structure of the novel nanoporous tin(iv) sulfide material tpa-sns-3," *Chemistry of Materials*, vol. 7, no. 2, pp. 245 – 248, 1995.
- [111] T. Jiang, A. Lough, G. A. Ozin, R. L. Bedard, and R. Broach, "Synthesis and structure of microporous layered tin(iv) sulfide materials," *J. Mater. Chem.*, vol. 8, pp. 721 – 732, 1998.
- [112] T. Jiang and G. A. Ozin, "New directions in tin sulfide materials chemistry," *J. Mater. Chem.*, vol. 8, pp. 1099 – 1108, 1998.
- [113] J. B. Parise, Y. Ko, J. Rijssenbeek, D. M. Nellis, K. Tan, and S. Koch, "Novel layered sulfides of tin: synthesis, structural characterization and ion exchange properties of tma-sns-1, $\text{sn}_3\text{s}_7 \cdot (\text{nme}_4)_2 \cdot \text{h}_2\text{o}$," *J. Chem. Soc., Chem. Commun.*, pp. 527 – 527, 1994.
- [114] C. L. Bowes, S. Petrov, G. Vovk, D. Young, G. A. Ozin, and R. L. Bedard, "Microporous layered tin sulfide, sns-1: molecular sieve or intercalant?," *J. Mater. Chem.*, vol. 8, pp. 711 – 720, 1998.
- [115] N. Pienack, D. Schinkel, A. Puls, M.-E. Ordolff, H. Lühmann, C. Näther, and W. Bensch, "New thioannates synthesized under solvothermal conditions: Crystal structures of $(\text{trenh})_2\text{sn}_3\text{s}_7$ and $[\text{Mn}(\text{tren})]_2\text{Sn}_2\text{S}_6$," *Zeitschrift für Naturforschung B*, vol. 67, no. 10, pp. 1098 – 1106, 2012.
- [116] M. Ø. Filsø, I. Chaaban, A. Al Shehabi, J. Skibsted, and N. Lock, "The structure-directing amine changes everything: structures and optical properties of two-dimensional thioannates," *Acta Crystallographica Section B*, vol. 73, pp. 931 – 940, Oct 2017.
- [117] X.-H. Qi, K.-Z. Du, M.-L. Feng, J.-R. Li, C.-F. Du, B. Zhang, and X.-Y. Huang, "A two-dimensionally microporous thioannate with superior cs^+ and sr^{2+} ion-exchange property," *Journal of Materials Chemistry A*, vol. 3, no. 10, pp. 5665 – 5673, 2015.
- [118] J. Han, L. Zhang, S. Li, W. Zheng, D. Jia, and Y. Yuan, "Alcohol-solvothermal syntheses, crystal structures and photocatalytic properties of tin selenides with polyselenide ligands," *CrystEngComm*, vol. 21, pp. 1642 – 1652, 2019.
- [119] R.-C. Zhang, C. Zhang, D.-J. Zhang, J.-J. Wang, Z.-F. Zhang, M. Ji, and Y.-L. An, "Copper-rich framework selenoarsenates based on icosahedral $\text{Cu}_8\text{Se}_{13}$ clusters," *Zeitschrift für anorganische und allgemeine Chemie*, vol. 638, no. 15, pp. 2503 – 2507, 2012.
- [120] M. Luo, D. Hu, H. Yang, D. Li, and T. Wu, "Pcu-type copper-rich open-framework chalcogenides: pushing up the length limit of the connection mode and the first mixed-metal $[\text{Cu}_7\text{GeSe}_{13}]$ cluster," *Inorg. Chem. Front.*, vol. 4, pp. 387 – 392, 2017.

- [121] G. L. Schimek, J. W. Kolis, and G. J. Long, “Metal hexaammine as a bulky cation: structural and property studies of $[m(\text{nh}_3)_6]\text{cu}_8\text{sb}_3\text{s}_{13}$ ($m = \text{mn, fe, ni}$) and $[\text{fe}(\text{nh}_3)_6]\text{ages}_4$ ($e = \text{as, sb}$),” *Chemistry of Materials*, vol. 9, no. 12, pp. 2776 – 2785, 1997.
- [122] Z. Zhang, J. Zhang, T. Wu, X. Bu, and P. Feng, “Three-dimensional open framework built from cus icosahedral clusters and its photocatalytic property,” *Journal of the American Chemical Society*, vol. 130, no. 46, pp. 15238 – 15239, 2008.
- [123] R.-C. Zhang, H.-G. Yao, S.-H. Ji, M.-C. Liu, M. Ji, and Y.-L. An, “Copper-rich framework sulfides: $\text{A}_4\text{cu}_8\text{ge}_3\text{s}_{12}$ ($a = \text{k, rb}$) with cubic perovskite structure,” *Inorganic Chemistry*, vol. 49, no. 14, pp. 6372 – 6374, 2010. PMID: 20565081.
- [124] R.-C. Zhang, C. Zhang, S.-H. Ji, M. Ji, and Y.-L. An, “Synthesis and characterization of $(\text{h}_2\text{dab})_2\text{cu}_8\text{ge}_4\text{s}_{14}\cdot 2\text{h}_2\text{o}$: An expanded framework based on icosahedral cu_8s_{12} cluster,” *Journal of Solid State Chemistry*, vol. 186, pp. 94 – 98, 2012.
- [125] S. Tang, J. Zhou, X. Liu, and H.-P. Xiao, “A new 3-d cuprous thiogermanate with rare 3-d $[\text{cu-s-cu}]_n$ network,” *Materials Today Communications*, vol. 15, pp. 88 – 93, 2018.
- [126] R.-C. Zhang, H.-G. Yao, S.-H. Ji, M.-C. Liu, M. Ji, and Y.-L. An, “ $(\text{h}_2\text{en})_2\text{cu}_8\text{sn}_3\text{s}_{12}$: a trigonal cus₃-based open-framework sulfide with interesting ion-exchange properties,” *Chem. Commun.*, vol. 46, pp. 4550 – 4552, 2010.
- [127] M. Behrens, M.-E. Ordolff, C. Näther, W. Bensch, K.-D. Becker, C. Guillot-Deudon, A. Lafond, and J. A. Cody, “New three-dimensional thiostrannates composed of linked cu_8s_{12} clusters and the first example of a mixed-metal $\text{cu}_7\text{sn}_3\text{s}_{12}$ cluster,” *Inorganic Chemistry*, vol. 49, no. 18, pp. 8305 – 8309, 2010. PMID: 20726515.
- [128] H. Yang, L. Wang, D. Hu, J. Lin, L. Luo, H. Wang, and T. Wu, “A novel copper-rich open-framework chalcogenide constructed from octahedral cu_4se_6 and icosahedral $\text{cu}_8\text{se}_{13}$ nanoclusters,” *Chem. Commun.*, vol. 52, pp. 4140 – 4143, 2016.
- [129] Y.-L. Wang, B. Zhang, W.-A. Li, M.-L. Feng, and X.-Y. Huang, “Two new 3d heterometallic chalcogenides based on copper-rich selenogermanate clusters,” *Inorganic Chemistry Communications*, vol. 85, pp. 41 – 44, 2017. Special issue for the 7th National Conference on Structural Chemistry of Chinese Chemical Society (2016, Guangzhou).
- [130] A. K. Cheetham, G. Férey, and T. Loiseau, “Open-Framework Inorganic Materials,” *Angewandte Chemie International Edition*, vol. 38, pp. 3268 – 3292, 11 1999.
- [131] J. Lin, Y. Dong, Q. Zhang, D. Hu, N. Li, Le Wang, Y. Liu, and T. Wu, “Interrupted chalcogenide-based zeolite-analogue semiconductor: atomically precise doping for tunable electro-/photoelectrochemical properties,” *Angewandte Chemie (International ed. in English)*, vol. 54, no. 17, pp. 5103 – 5107, 2015.

- [132] C. Xue, D. Hu, Y. Zhang, H. Yang, X. Wang, W. Wang, and T. Wu, “Two unique crystalline semiconductor zeolite analogues based on indium selenide clusters,” *Inorganic Chemistry*, vol. 56, no. 24, pp. 14763 – 14766, 2017. PMID: 29199823.
- [133] C. L. Cahill and J. B. Parise, “Synthesis and structure of $\text{mng}_4\text{s}_{10}(\text{c}_6\text{h}_{14}\text{n}_2)\cdot 3\text{h}_2\text{o}$: a novel sulfide framework analogous to zeolite li-a(bw),” *Chemistry of Materials*, vol. 9, no. 3, pp. 807 – 811, 1997.
- [134] Q. Lin, X. Bu, C. Mao, X. Zhao, K. Sasan, and P. Feng, “Mimicking high-silica zeolites: Highly stable germanium- and tin-rich zeolite-type chalcogenides,” *Journal of the American Chemical Society*, vol. 137, no. 19, pp. 6184 – 6187, 2015. PMID: 25950820.
- [135] X. Chen, X. Bu, Q. Lin, C. Mao, Q. Zhai, Y. Wang, and P. Feng, “Selective Ion Exchange and Photocatalysis by Zeolite-Like Semiconducting Chalcogenide,” *Chemistry – A European Journal*, vol. 23, pp. 11913 – 11919, 9 2017.
- [136] Z. Wu, X.-L. Wang, D. Hu, S. Wu, C. Liu, X. Wang, R. Zhou, D.-S. Li, and T. Wu, “A new cluster-based chalcogenide zeolite analogue with a large inter-cluster bridging angle,” *Inorg. Chem. Front.*, vol. 6, pp. 3063 – 3069, 2019.
- [137] X. Chen, X. Bu, Y. Wang, Q. Lin, and P. Feng, “Charge- and Size-Complementary Multimetal-Induced Morphology and Phase Control in Zeolite-Type Metal Chalcogenides,” *Chemistry – A European Journal*, vol. 24, pp. 10812 – 10819, 7 2018.
- [138] N. Zheng, X. Bu, B. Wang, and P. Feng, “Synthetic design of crystalline inorganic chalcogenides exhibiting fast-ion conductivity,” *Nature*, vol. 426, p. 428 – 432, 2003.
- [139] N. Zheng, X. Bu, and P. Feng, “ $\text{Na}_5(\text{in}_4\text{s})(\text{ins}_4)_3\cdot 6\text{h}_2\text{o}$, a zeolite-like structure with unusual sin_4 tetrahedra,” *Journal of the American Chemical Society*, vol. 127, no. 15, pp. 5286 – 5287, 2005. PMID: 15826143.
- [140] P. Vaqueiro, “Hybrid materials through linkage of chalcogenide tetrahedral clusters,” *Dalton Trans.*, vol. 39, pp. 5965 – 5972, 2010.
- [141] I. G. Dance, “Formation, crystal structure, and reactions of $\text{catena}-(\mu\text{-sph})[(\mu\text{-sph})_6\text{zn}_4(\text{ch}_3\text{oh})(\text{sph})]$, a model for zinc thiolate metalloenzymes,” *Journal of the American Chemical Society*, vol. 102, no. 10, pp. 3445 – 3451, 1980.
- [142] G. A. Casagrande, E. S. Lang, G. M. de Oliveira, M. Hörner, and F. Broch, “Dealing with 1,3-bis(4-nitrophenyl)triazene as intermediary ligand in the synthesis of polymeric $(\mu\text{-se})\text{hg}$ -clusters: One-pot synthetic procedures and x-ray structural characterization of $[(\text{phse})_7\text{hg}_4\text{brpy}]_n$,” *Inorganica Chimica Acta*, vol. 360, no. 5, pp. 1776 – 1779, 2007.
- [143] I. G. Dance, R. G. Garbutt, D. C. Craig, M. L. Scudder, and T. D. Bailey, “New non-molecular poly-adamantanoid crystal structures of $\text{cd}(\text{sar})_2$, zeolitic $\text{cd}_4(\text{sc}_6\text{h}_4\text{me-4})_8$, and solvated $\text{cd}_8(\text{sc}_6\text{h}_4\text{br-4})_{16}(\text{dmf})_3$ (dmf = dimethylformamide), in relation to the molecular

- structures of aggregates in solution,” *J. Chem. Soc., Chem. Commun.*, pp. 1164 – 1167, 1987.
- [144] I. G. Dance, R. G. Garbutt, D. C. Craig, and M. L. Scudder, “The different non- molecular polyadamantanoid crystal structures of cadmium benzenethiolate and 4-methylbenzenethiolate. analogies with microporous aluminosilicate frameworks,” *Inorganic Chemistry*, vol. 26, no. 24, pp. 4057 – 4064, 1987.
- [145] K. Anjali and J. J. Vittal, “Polylinked adamantanoid structure of cd(seph)₂,” *Inorganic Chemistry Communications*, vol. 3, no. 12, pp. 708 – 710, 2000.
- [146] Q. Zhang, X. Bu, J. Zhang, T. Wu, and P. Feng, “Chiral semiconductor frameworks from cadmium sulfide clusters,” *Journal of the American Chemical Society*, vol. 129, no. 27, pp. 8412 – 8413, 2007. PMID: 17567135.
- [147] Q. Zhang, Z. Lin, X. Bu, T. Wu, and P. Feng, “Solvothermal conversion of discrete cubic cadmium thiolate cluster into supertetrahedral cluster decorating quartz-type chiral superlattice,” *Chemistry of Materials*, vol. 20, no. 10, pp. 3239 – 3241, 2008.
- [148] Q. Zhang, Y. Liu, X. Bu, T. Wu, and P. Feng, “A Rare (3,4)-Connected Chalcogenide Superlattice and Its Photoelectric Effect,” *Angewandte Chemie International Edition*, vol. 47, no. 1, pp. 113 – 116, 2007.
- [149] N. Zheng, H. Lu, X. Bu, and P. Feng, “Metal-chelate dye-controlled organization of cd₃₂s₁₄(sph)₄₀₄- nanoclusters into three-dimensional molecular and covalent open architecture,” *Journal of the American Chemical Society*, vol. 128, no. 14, pp. 4528 – 4529, 2006. PMID: 16594662.
- [150] T. Wu, X. Bu, P. Liao, L. Wang, S.-T. Zheng, R. Ma, and P. Feng, “Superbase route to supertetrahedral chalcogenide clusters,” *Journal of the American Chemical Society*, vol. 134, no. 8, pp. 3619 – 3622, 2012. PMID: 22335388.
- [151] P. Vaqueiro and M. L. Romero, “[ga₁₀s₁₆(nc₇h₉)₄]₂: a hybrid supertetrahedral nanocluster,” *Chem. Commun.*, pp. 3282 – 3284, 2007.
- [152] J. Xie, X. Bu, N. Zheng, and P. Feng, “One-dimensional coordination polymers containing penta-supertetrahedral sulfide clusters linked by dipyridyl ligands,” *Chem. Commun.*, pp. 4916 – 4918, 2005.
- [153] N. Zheng, X. Bu, H. Lu, L. Chen, and P. Feng, “One-dimensional assembly of chalcogenide nanoclusters with bifunctional covalent linkers,” *Journal of the American Chemical Society*, vol. 127, no. 43, pp. 14990 – 14991, 2005. PMID: 16248614.
- [154] Q. Zhang, X. Bu, Z. Lin, T. Wu, and P. Feng, “Organization of tetrahedral chalcogenide clusters using a tetrahedral quadridentate linker,” *Inorganic Chemistry*, vol. 47, no. 21, pp. 9724 – 9726, 2008. PMID: 18828584.

- [155] N. Zheng, X. Bu, J. Lauda, and P. Feng, “Zero- and two-dimensional organization of tetrahedral cadmium chalcogenide clusters with bifunctional covalent linkers,” *Chemistry of Materials*, vol. 18, no. 18, pp. 4307 – 4311, 2006.
- [156] C. Xu, Y.-G. Han, T. Duan, Q.-F. Zhang, and W.-H. Leung, “Two-dimensional assembly of the type $\text{Cd}_{10}\text{Te}_4$ thiolate cluster with 4,4-trimethylenedipyridine,” *Inorganic Chemistry Communications*, vol. 12, no. 10, pp. 1053 – 1056, 2009.
- [157] Z. Chen, D. Luo, X. Luo, M. Kang, and Z. Lin, “Two-dimensional assembly of tetrahedral chalcogenide clusters with tetrakis(imidazolyl)borate ligands,” *Dalton Trans.*, vol. 41, pp. 3942 – 3944, 2012.
- [158] P. Vaqueiro and M. L. Romero, “Gallium sulfide supertetrahedral clusters as building blocks of covalent organico-inorganic networks,” *Journal of the American Chemical Society*, vol. 130, no. 30, pp. 9630 – 9631, 2008. PMID: 18597468.
- [159] P. Vaqueiro, R. M. B. Rowan, and B. Richards, “Arrays of Chiral Nanotubes and a Layered Coordination Polymer Containing Gallium – Sulfide Supertetrahedral Clusters,” *Chemistry - A European Journal*, vol. 16, no. 15, pp. 4462 – 4465, 2010.
- [160] P. Vaqueiro, S. Makin, Y. Tong, and S. J. Ewing, “A new class of hybrid super-supertetrahedral cluster and its assembly into a five-fold interpenetrating network,” *Dalton Trans.*, vol. 46, pp. 3816 – 3819, 2017.
- [161] M. J. Manos, J. I. Jang, J. B. Ketterson, and M. G. Kanatzidis, “[$\text{Zn}(\text{H}_2\text{O})_4$][$\text{Zn}_2\text{Sn}_3\text{Se}_9(\text{menH}_2)$]: a robust open framework chalcogenide with a large nonlinear optical response,” *Chem. Commun.*, pp. 972 – 974, 2008.
- [162] T. Wu, R. Khazhakyann, L. Wang, X. Bu, S. Zheng, V. Chau, and P. Feng, “Three- Dimensional Covalent Co-Assembly between Inorganic Supertetrahedral Clusters and Imidazolates,” *Angewandte Chemie International Edition*, vol. 50, no. 11, pp. 2536 – 2539, 2011.
- [163] J. Zhang, W. Wang, C. Xue, M. Zhao, D. Hu, J. Lv, X. Wang, D. Li, and T. Wu, “Metal chalcogenide imidazolate frameworks with hybrid intercluster bridging mode and unique interrupted topological structure,” *Inorganic Chemistry*, vol. 57, no. 16, pp. 9790 – 9793, 2018. PMID: 30074779.
- [164] Y. Hou, T. Wu, Le Wang, and P. Feng, “Integration of supertetrahedral cluster with reduced graphene oxide sheets for enhanced photostability and photoelectrochemical properties,” *Science China Chemistry*, vol. 56, no. 4, pp. 423 – 427, 2013.
- [165] Z.-Q. Li, C.-J. Mo, Y. Guo, N.-N. Xu, Q.-Y. Zhu, and J. Dai, “Discrete supertetrahedral clusters nanoclusters and their application in fabrication of cluster-sensitized TiO_2 photoelectrodes,” *J. Mater. Chem. A*, vol. 5, pp. 8519 – 8525, 2017.

- [166] D. Liu, P. Huang, Y. Liu, Z. Wu, D. Li, J. Guo, and T. Wu, "Cd/in-codoped tio₂ nanochips for high-efficiency photocatalytic dye degradation," *Dalton Trans.*, vol. 47, pp. 6177 – 6183, 2018.
- [167] D. Liu, Y. Liu, P. Huang, C. Zhu, Z. Kang, J. Shu, M. Chen, X. Zhu, J. Guo, L. Zhuge, X. Bu, P. Feng, and T. Wu, "Highly Tunable Heterojunctions from Multimetallic Sulfide Nanoparticles and Silver Nanowires," *Angewandte Chemie International Edition*, vol. 57, no. 19, pp. 5374 – 5378, 2018.
- [168] R. Hu, X.-L. Wang, J. Zhang, D. Hu, J. Wu, R. Zhou, L. Li, M. Li, D.-S. Li, and T. Wu, "Multi – metal nanocluster assisted cu – ga – sn tri – doping for enhanced photoelectrochemical water splitting of bivo 4 film," *Advanced Materials Interfaces*, p. 2000016, 2020.
- [169] C. Mao, Y. Wang, W. Jiao, X. Chen, Q. Lin, M. Deng, Y. Ling, Y. Zhou, X. Bu, and P. Feng, "Integrating zeolite-type chalcogenide with titanium dioxide nanowires for enhanced photoelectrochemical activity," *Langmuir*, vol. 33, no. 47, pp. 13634 – 13639, 2017. PMID: 29139299.
- [170] D.-D. Hu, J. Lin, Q. Zhang, J.-N. Lu, X.-Y. Wang, Y.-W. Wang, F. Bu, L.-F. Ding, L. Wang, and T. Wu, "Multi-step host – guest energy transfer between inorganic chalcogenide-based semiconductor zeolite material and organic dye molecules," *Chemistry of Materials*, vol. 27, no. 11, pp. 4099 – 4104, 2015.
- [171] D.-D. Hu, L. Wang, J. Lin, F. Bu, and T. Wu, "Tuning the efficiency of multi-step energy transfer in a host – guest antenna system based on a chalcogenide semiconductor zeolite through acidification and solvation of guests," *J. Mater. Chem. C*, vol. 3, pp. 11747 – 11753, 2015.
- [172] D. Hu, X. Wang, H. Yang, D. Liu, Y. Wang, J. Guo, and T. Wu, "Host-guest electrocatalyst with cage-confined cuprous sulfide nanoparticles in etched chalcogenide semiconductor zeolite for highly efficient oxygen reduction reaction," *Electrochimica Acta*, vol. 282, pp. 877 – 885, 2018.
- [173] P. Walden, "Molecular weights and electrical conductivity of several fused salts," *Bulletin of the Imperial Academy of Sciences (Saint Petersburg)*, vol. 1800, p. 405 – 422, 1914.
- [174] R. D. Rogers and K. R. Seddon, "Ionic liquids – solvents of the future?," *Science*, vol. 302, no. 5646, pp. 792 – 793, 2003.
- [175] E. R. Parnham and R. E. Morris, "Ionothermal synthesis of zeolites, metal – organic frameworks, and inorganic – organic hybrids," *Accounts of Chemical Research*, vol. 40, no. 10, pp. 1005 – 1013, 2007. PMID: 17580979.
- [176] D. Freudenmann, S. Wolf, M. Wolff, and C. Feldmann, "Ionic liquids: new perspectives for inorganic synthesis?," *Angewandte Chemie (International ed. in English)*, vol. 50, no. 47, pp. 11050 – 11060, 2011.

- [177] “Ionic liquids and eutectic mixtures as solvent and template in synthesis of zeolite analogues,” *Nature*, vol. 430, pp. 1012 – 1016, 2004.
- [178] W.-W. Xiong, J.-R. Li, B. Hu, B. Tan, R.-F. Li, and X.-Y. Huang, “Largest discrete supertetrahedral clusters synthesized in ionic liquids,” *Chem. Sci.*, vol. 3, pp. 1200 – 1204, 2012.
- [179] Y. Lin, W. Massa, and S. Dehnen, ““zeoball” $[\text{sn}_3\text{ge}_2\text{se}_3]_{24}^-$: A molecular anion with zeolite-related composition and spherical shape,” *Journal of the American Chemical Society*, vol. 134, no. 10, pp. 4497 – 4500, 2012. PMID: 22369242.
- [180] N.-N. Shen, B. Hu, C.-C. Cheng, G.-D. Zou, Q.-Q. Hu, C.-F. Du, J.-R. Li, and X.-Y. Huang, “Discrete supertetrahedral t_3 inq clusters ($q = s, s/se, se, se/te$): Ionothermal syntheses and tunable optical and photodegradation properties,” *Crystal Growth & Design*, vol. 18, no. 2, pp. 962 – 968, 2018.
- [181] M. Hao, Q. Hu, Y. Zhang, M. Luo, Y. Wang, B. Hu, J. Li, and X. Huang, “Soluble supertetrahedral chalcogenide t_4 clusters: High stability and enhanced hydrogen evolution activities,” *Inorganic Chemistry*, vol. 58, no. 8, pp. 5126 – 5133, 2019.
- [182] Y. Wang, Z. Zhu, Z. Sun, Q. Hu, J. Li, J. Jiang, and X. Huang, “Discrete supertetrahedral t_5 selenide clusters and their se/s solid solutions: Ionic-liquid-assisted precursor route syntheses and photocatalytic properties,” *Chemistry (Weinheim an der Bergstrasse, Germany)*, vol. 26, no. 7, pp. 1624 – 1632, 2020.
- [183] S. Santner and S. Dehnen, “[$m_4\text{sn}_4\text{se}_7$] $_{10}^-$ cluster anions ($m = \text{mn, zn, cd}$) in a cs^+ environment and as ternary precursors for ionothermal treatment,” *Inorganic Chemistry*, vol. 54, no. 4, pp. 1188 – 1190, 2015. PMID: 25622069.
- [184] J.-R. Li, Z.-L. Xie, X.-W. He, L.-H. Li, and X.-Y. Huang, “Crystalline open-framework selenidostannates synthesized in ionic liquids,” *Angewandte Chemie (International ed. in English)*, vol. 50, no. 48, pp. 11395 – 11399, 2011.
- [185] Y. Lin and S. Dehnen, “[bmim] $_4[\text{sn}_9\text{se}_{20}]$: Ionothermal synthesis of a selenidostannate with a 3d open-framework structure,” *Inorganic Chemistry*, vol. 50, no. 17, pp. 7913 – 7915, 2011. PMID: 21809815.
- [186] Y. Lin, D. Xie, W. Massa, L. Mayrhofer, S. Lippert, B. Ewers, A. Chernikov, M. Koch, and S. Dehnen, “Changes in the structural dimensionality of selenidostannates in ionic liquids: Formation, structures, stability, and photoconductivity,” *Chemistry – A European Journal*, vol. 19, no. 27, pp. 8806 – 8813, 2013.
- [187] Y. Lin, W. Massa, and S. Dehnen, “Controlling the assembly of chalcogenide anions in ionic liquids: From binary ge/se through ternary $ge/sn/se$ to binary sn/se frameworks,” *Chemistry – A European Journal*, vol. 18, no. 42, pp. 13427 – 13434, 2012.

- [188] J.-R. Li, W.-W. Xiong, Z.-L. Xie, C.-F. Du, G.-D. Zou, and X.-Y. Huang, "From selenidostannates to silver-selenidostannate: structural variation of chalcogenidometallates synthesized in ionic liquids," *Chem. Commun.*, vol. 49, pp. 181 – 183, 2013.
- [189] C.-F. Du, J.-R. Li, M.-L. Feng, G.-D. Zou, N.-N. Shen, and X.-Y. Huang, "Varied forms of lamellar $[\text{sn}_3\text{se}_7]_n^{2n-}$ anion: the competitive and synergistic structure-directing effects of metal – amine complex and imidazolium cations," *Dalton Trans.*, vol. 44, pp. 7364 – 7372, 2015.
- [190] S. Santner, J. A. P. Sprenger, M. Finze, and S. Dehnen, "The role of $[\text{bf}_4]$ and $[\text{b}(\text{cn})_4]$ anions in the ionothermal synthesis of chalcogenidometallates," *Chemistry – A European Journal*, vol. 24, no. 14, pp. 3474 – 3480, 2018.
- [191] W.-W. Xiong, G. Zhang, and Q. Zhang, "New strategies to prepare crystalline chalcogenides," *Inorg. Chem. Front.*, vol. 1, pp. 292 – 301, 2014.
- [192] W. Xiong and Q. Zhang, "Surfactants as Promising Media for the Preparation of Crystalline Inorganic Materials," *Angewandte Chemie International Edition*, vol. 54, no. 40, pp. 11616 – 11623, 2015.
- [193] J. Li, L. Delmotte, and H. Kessler, "Synthesis and characterization of a novel mesostructured layered tin(IV) sulfide," *Chem. Commun.*, pp. 1023 – 1024, 1996.
- [194] J. Li, H. Kessler, and L. Delmotte, "Study of novel mesostructured materials based on tin(IV) sulfide part 1.—synthesis and characterization," *J. Chem. Soc., Faraday Trans.*, vol. 93, pp. 665 – 668, 1997.
- [195] J. Li, B. Marler, H. Kessler, M. Soulard, and S. Kallus, "Synthesis, structure analysis, and characterization of a new thiostannate, $(\text{c}_{12}\text{h}_{25}\text{nh}_3)_4[\text{sn}_2\text{s}_6]\cdot 2\text{h}_2\text{o}$," *Inorganic Chemistry*, vol. 36, no. 21, pp. 4697 – 4701, 1997. PMID: 11670146.
- [196] F. Bonhomme and M. G. Kanatzidis, "Structurally characterized mesostructured hybrid surfactant/inorganic lamellar phases containing the adamantane $[\text{ge}_4\text{s}_{10}]_4^-$ anion: synthesis and properties," *Chemistry of Materials*, vol. 10, no. 4, pp. 1153 – 1159, 1998.
- [197] M. J. MacLachlan, N. Coombs, and G. A. Ozin, "Non-aqueous supramolecular assembly of mesostructured metal germanium sulphides from $(\text{Ge}_4\text{S}_{10})_4$ clusters," *Nature*, vol. 397, pp. 681 – 684, 1999.
- [198] K. K. Rangan and M. G. Kanatzidis, "Mesolamellar thiogermanates $[\text{c}_{nh}2n+1\text{nh}_3]_4\text{ge}_4\text{s}_{10}$," *Inorganica Chimica Acta*, vol. 357, no. 13, pp. 4036 – 4044, 2004. Protagonist in Chemistry: Tobin J. Marks.
- [199] M. Wachhold and M. G. Kanatzidis, "Surfactant-templated inorganic lamellar and non-lamellar hybrid phases containing adamantane $[\text{ge}_4\text{se}_{10}]_4^-$ anions," *Chemistry of Materials*, vol. 12, no. 10, pp. 2914 – 2923, 2000.

- [200] A. Eichhöfer, O. Hampe, and M. Blom, "Synthesis, Structures, and Properties of a Series of $[\text{Cd}_8\text{Se}(\text{SePh})_{12}\text{Cl}_4]_2$ Cluster Compounds with Different Counterions," *European Journal of Inorganic Chemistry*, vol. 2003, no. 7, pp. 1307 – 1314, 2003.
- [201] W.-W. Xiong, E. U. Athresh, Y. T. Ng, J. Ding, T. Wu, and Q. Zhang, "Growing crystalline chalcogenidoarsenates in surfactants: From zero-dimensional cluster to three-dimensional framework," *Journal of the American Chemical Society*, vol. 135, no. 4, pp. 1256 – 1259, 2013. PMID: 23311760.
- [202] W.-W. Xiong, P.-Z. Li, T.-H. Zhou, A. I. Y. Tok, R. Xu, Y. Zhao, and Q. Zhang, "Kinetically controlling phase transformations of crystalline mercury selenidostannates through surfactant media," *Inorganic Chemistry*, vol. 52, no. 8, pp. 4148 – 4150, 2013. PMID: 23556509.
- [203] J. Gao, Q. Tay, P.-Z. Li, W.-W. Xiong, Y. Zhao, Z. Chen, and Q. Zhang, "Surfactant-Thermal Method to Synthesize a Novel Two-Dimensional Oxochalcogenide," *Chemistry – An Asian Journal*, vol. 9, no. 1, pp. 131 – 134, 2014.
- [204] G. Zhang, P. Li, J. Ding, Y. Liu, W.-W. Xiong, L. Nie, T. Wu, Y. Zhao, A. I. Y. Tok, and Q. Zhang, "Surfactant-thermal syntheses, structures, and magnetic properties of $\text{mn-ge-sulfides/selenides}$," *Inorganic Chemistry*, vol. 53, no. 19, pp. 10248 – 10256, 2014. PMID: 25208101.
- [205] Y. Shen, C. Liu, P. Hou, M. Zhi, C. Zhou, W. Chai, J. Cheng, Y. Liu, and Q. Zhang, "Preparation of Porous Three-Dimensional Quaternary Thioantimonates(III) ACuSb_2S_4 ($\text{A}=\text{Rb}, \text{Cs}$) through a Surfactant-Thermal Method," *Chemistry – An Asian Journal*, vol. 10, no. 12, pp. 2604 – 2608, 2015.
- [206] W. Xiong, J. Miao, K. Ye, Y. Wang, B. Liu, and Q. Zhang, "Threading Chalcogenide Layers with Polymer Chains," *Angewandte Chemie International Edition*, vol. 54, no. 2, pp. 546 – 550, 2015.